

# Ultrasonic bubble chambers

V. A. Akulichev

*Acoustics Institute, Academy of Sciences of the USSR, Moscow*

V. A. Zhukov and L. G. Tkachev

*Joint Institute for Nuclear Research, Dubna*

*Fiz. Élem. Chastits At. Yadra 8, 580-630 (May-June, 1977)*

The results of theoretical and experimental investigations of the problem of making ultrasonic bubble chambers (USBCs) are reviewed. The main facts and results so far accumulated are presented.

PACS numbers: 29.40.Fw

## INTRODUCTION

One of the most important instruments in high energy physics—the bubble chamber—has two serious shortcomings: First, it is a slow instrument, as a result of which one effectively uses only an insignificant part of the time during which the chamber is exposed to the particle beam; second, in a bubble chamber one cannot use electronic systems to select particular events of interest because of the exceptionally short lifetime of the bubbles once formed. While it is virtually impossible to eliminate the second difficulty, since it is due to physical reasons, it is a technically feasible problem to increase the repetition rate of the chambers to tens and hundreds of cycles per second by means of expansion systems constructed on the basis of new principles.

Recently, there has been a considerable increase in the interest in chambers with high repetition rate in connection with the development of so-called hybrid instruments<sup>1</sup> intended for experiments with large accelerators. These instruments include one or several bubble chambers and also systems of electronic detectors working in conjunction with a computer. The efficiency with which these instruments can be used is largely determined by the repetition rate of their bubble chambers.

A bubble chamber with high repetition rate can, for example, be constructed along the lines of the resonance chamber described in Ref. 2, in which the components of the expansion system and the liquid itself form a resonant system, or along the lines of a chamber with an electrodynamic expansion system,<sup>2</sup> in which the driving element has a coil placed in a magnetic field and excited by an alternating current.

There is also one further possibility of increasing the repetition rate of a bubble chamber. In some studies, it was found that the sensitivity of various liquids to ionizing radiation is affected when an ultrasonic field is applied to them. After investigation, attempts were made to use ultrasound to detect the tracks of ionizing particles, positive results being obtained only recently. The experimental data demonstrated the basic possibility of making ultrasonic bubble chambers with high repetition rate, and theoretical investigations have provided rich material for understanding the mechanism of growth of the incipient bubbles formed in the liquid by the ionizing radiation under the influence of the ultrasonic field.

## 1. INVESTIGATION OF THE INFLUENCE OF IONIZING RADIATION ON A LIQUID TO WHICH AN ULTRASONIC FIELD IS APPLIED

### Cavitation nuclei and cavitation strength of liquids

In liquids that have not been especially purified, there are always phase inclusions that reduce their strength; these are usually called nucleating centers of a new phase or cavitation nuclei. They may take the form of gas bubbles, solid unwettable particles, or vapor bubbles produced by local heat sources when the liquids are heated to temperatures near the boiling point. Vapor bubbles can also arise as a result of interaction of ionizing particles with the liquid. However, their characteristic sizes<sup>4</sup> are too small ( $10^{-6}$ – $10^{-7}$  cm) compared with the sizes of the nucleating bubbles associated with impurities ( $10^{-3}$ – $10^{-4}$  cm), which determine the breaking strength of such liquids, while the influence of the ionizing radiation is insignificant.<sup>5-7</sup>

The working liquids used in bubble chambers are as a rule carefully purified of solid and gaseous impurities, so that their strength is primarily determined by the vapor cavitation nuclei. Cryogenic liquids are distinguished by particular purity. For example, liquid hydrogen in the uncondensed gaseous state can contain only helium, whose concentration is usually reduced to a negligible amount. It is fundamentally impossible for liquid helium to contain any uncondensed dissolved gases or gaseous cavitation nuclei associated with them.

According to the ideas developed by Seitz,<sup>4</sup> the formation of nucleating bubbles by ionizing particles in liquids under the conditions of operation of bubble chambers occurs as a result of the secondary ionization produced by  $\delta$  electrons. As a result of the transformation of the energy loss of the  $\delta$  electrons into heat, a certain volume of the liquid with characteristic radius  $R_h$  is heated, and after evaporation this is transformed into a spherical bubble of radius  $R_0$  (Ref. 8):

$$R_0 \approx R_h(\rho/\rho')^{1/3}, \quad (1)$$

where  $\rho$  is the density of the liquid;  $\rho'$  is the density of the vapor in the bubble. The bubble then grows and may reach a size that makes it visible if  $R_0$  is greater than a certain critical  $R_{cr}$ ; otherwise it collapses. The time taken by the bubble to grow to the critical size is deter-

mined by the diffusion of heat from its cavity and is, according to estimates,<sup>4,9</sup> about  $10^{-10}$  sec. Cavitation fracture of a liquid is always due to the formation of bubbles of the critical size  $R_{cr}$ , which is determined by the condition

$$p'(R, T) = p_{cr} + 2\sigma/R_{cr}, \quad (2)$$

where  $\sigma$  is the surface tension of the liquid;  $p'$  is the pressure of the vapor in the bubble, which depends on its radius  $R$  and the temperature  $T$  of the liquid;  $p_{cr}$  is the threshold pressure in the liquid above which the bubble begins to grow. Using the connection between  $p'(R, T)$  and the saturated vapor pressure  $p'_s(T)$  on a plane liquid-vapor boundary expressed in the form

$$p'(R, T) = p'_s(T) - \frac{2\sigma}{R} \frac{\rho'}{\rho - \rho'}, \quad (3)$$

we can transform Eq. (2) to the most convenient form, in which the value of the critical radius  $R_{cr}$  is determined by the vapor pressure above the plane vapor-liquid surface  $p'_s(T) = p_{cr}(T)$  and by the pressure  $p_{cr}$  in the liquid:

$$R_{cr} = 2\sigma / [(p_{cr} - p'_s)(1 - \rho'/\rho)]. \quad (4)$$

The energy needed for the formation of a vapor bubble of critical radius  $R_{cr}$  can be expressed in the form<sup>8</sup>

$$E_{cr} = E'_{cr} + E''_{cr}, \quad (5)$$

where  $E'_{cr}$  characterizes the reversible energy expenditure and  $E''_{cr}$  the irreversible. The value of  $E'_{cr}$  is determined by the energy used for evaporation, and also by the minimal work of formation of the cavity due to the surface and volume energies:

$$E'_{cr} = (4/3)\pi R_{cr}^3 \rho' L + 4\pi R_{cr}^2 (\sigma - T d\sigma/dT) - (p_{cr} - p'_s)(4/3)\pi R_{cr}^3 (1 - \rho'/\rho), \quad (6)$$

TABLE I. Working parameters of some liquids used in bubble chambers and characteristics of the ultrasonic field.

Parameters of liquid, characteristics of ultrasonic field	Hydrogen	Helium	Propane
$T_0$ , °K	27	4.2	333
$P_0$ , atm	4.8	1.0	22.0
$p_0 - p_{cr}$ , atm	2.0	0.25	10.0
$\rho$ , g/cm <sup>3</sup>	0.06	0.125	0.44
$\rho'$ , g/cm <sup>3</sup>	0.006	0.016	0.04
$\sigma$ , dyn/cm	0.8	0.1	3.6
$L$ , $10^{-9}$ erg/g	3.8	0.2	4.7
$R_{cr}$ , $10^{-6}$ cm	0.8	0.57	0.72
$E_{cr}$ , $10^{-12}$ erg	51	2.6	305
$E_{cr}$ , eV	32	1.6	190
$c$ , $10^5$ cm/sec	0.86	0.19	1.9
$\rho c$ , $10^5$ g·cm <sup>-2</sup> ·sec <sup>-1</sup>	0.05	0.025	0.83
$p_m$ , atm	3.0	0.3	10
$W$ , W/cm <sup>2</sup>	90	1.8	60

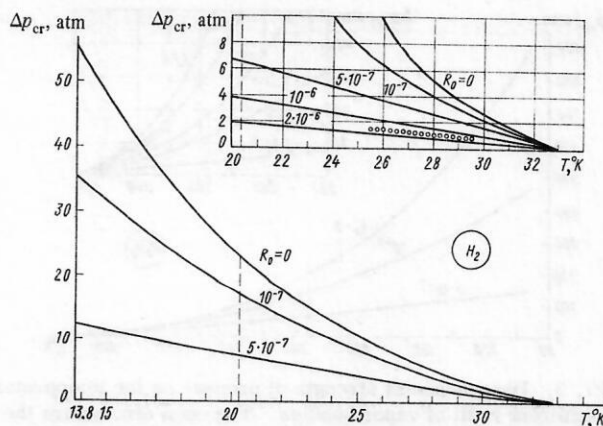


FIG. 1. Dependence of strength of liquid hydrogen on the temperature at different radii of vapor bubbles (Ref. 11). The open circles are the boundary of the region of sensitivity to ionizing radiation.<sup>8</sup>

where  $L$  is the heat of vaporization. The value of  $E''_{cr}$  is determined by the irreversible energy expenditure accompanying the growth of the cavity to the critical size and is associated with the inertia of the liquid, viscosity, and heat conduction, which are hard to take into account exactly. However,  $E'_{cr}$  is usually considerably larger<sup>8</sup> than  $E''_{cr}$ , and therefore the complete energy  $E_{cr}$  can be estimated by means of Eq. (6). As the estimates show,<sup>4,8,9</sup> if bubbles of critical radius are to be formed in liquids under the characteristic regimes of bubble chambers, there must be a local release of energy of tens to hundreds of electron volts.

For various regimes ( $T$ ,  $p_0 - p_{cr}$ ) of operation of hydrogen, helium, and propane bubble chambers, Table I contains the values of the critical radii  $R_{cr}$  and energies  $E_{cr}$  calculated in accordance with (4)–(6) using the tabulated<sup>10</sup> values of the thermodynamic parameters corresponding to the given temperatures.

To each value of the radius  $R_0$  of a vapor bubble in a

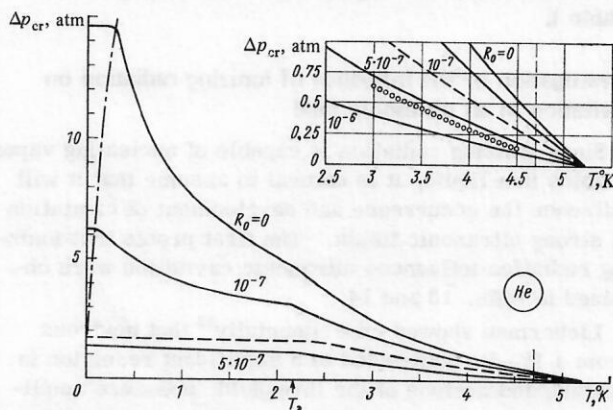


FIG. 2. Dependence of strength of liquid helium on the temperature at different radii of vapor bubbles.<sup>12</sup> The open circles are the boundary of the region of sensitivity to ionizing radiation<sup>8</sup>; the dashed curve is the strength determined by "electron bubbles"; the chain curve is the boundary of the region of quantum heterophase fluctuations.



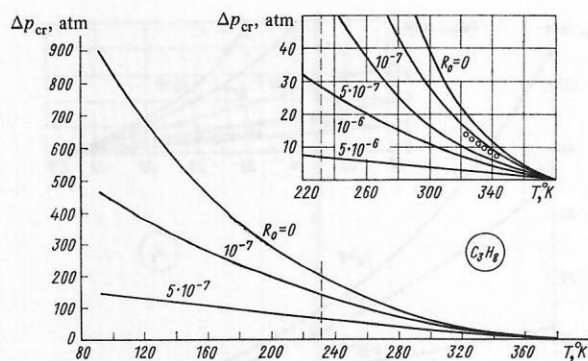


FIG. 3. Dependence of strength of propane on the temperature at different radii of vapor bubbles. The open circles are the boundary of the region of sensitivity to ionizing radiation.<sup>8</sup>

liquid there corresponds a minimal negative pressure  $p_\sigma - p_{cr}$  at which bubbles grow to visible size. One may call  $\Delta p_{cr} = p_\sigma - p_{cr}$  the fracture negative pressure, or cavitation strength, of the liquid. The dependence of  $\Delta p_{cr}$  on the temperature for different values of the radius  $R_0$  for hydrogen, helium, and propane<sup>11,12</sup> is given in Figs. 1–3.

These results refer to static stresses of liquids with a characteristic time of about  $10^{-2}$  sec, which appreciably exceeds the time of growth of bubbles to the critical size ( $\sim 10^{-10}$  sec). In an ultrasonic field with a frequency of the order of tens or hundreds of kilohertz, the characteristic stress times are also fairly long—about  $10^{-4}$ – $10^{-5}$  sec. Therefore, the threshold pressure amplitude  $p_{m,cr}$  of an ultrasonic field in an USBC can be estimated in the same way as the overpressure in ordinary chambers, i.e.,

$$p_{m,cr} \approx \Delta p_{cr} + \Delta p_0,$$

where  $\Delta p_{cr}$  is the cavitation strength of the liquid under static stress introduced above;  $\Delta p_0$  is the static overpressure of the liquid, i.e., the excess of the static pressure  $p_0$  over the saturated vapor pressure  $p_\sigma$ . The values of the characteristic acoustic parameters of ultrasonic fields and liquids for USBCs are given in Table I.

### Investigation of the influence of ionizing radiation on cavitation in an ultrasonic field

Since ionizing radiation is capable of nucleating vapor bubbles in a liquid, it is natural to assume that it will influence the occurrence and development of cavitation in strong ultrasonic fields. The first proofs that ionizing radiation influences ultrasonic cavitation were obtained in Refs. 13 and 14.

Lieberman showed experimentally<sup>13</sup> that neutrons from a Po–Be source led to a significant reduction in pentane and acetone of the threshold pressure amplitudes of the ultrasonic field  $p_{m,cr}$  at which cavitation occurs. At the same time, when these liquids were irradiated with positrons the effect was not observed. In these investigations, the cavitation was excited in degassed liquids in a 12-liter glass resonator. As a result of the degassing of the liquids, excitation in the

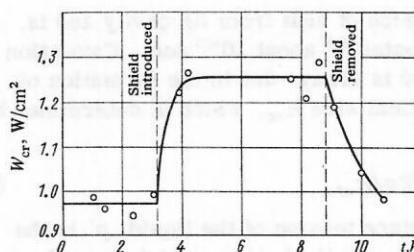


FIG. 4. Influence of lead shield on threshold intensity of an ultrasonic field in water.<sup>14</sup>

center of the resonator of the ultrasonic field with pressure amplitude greater than 22 atm did not lead to the occurrence of cavitation in the absence of a radioactive source. In the case of irradiation with neutrons, the cavitation strength was reduced so much that in pentane cavitation occurred when the ultrasonic field had an amplitude 3.5 atm, and in acetone when it was 6.5 atm. Lieberman suggested<sup>13</sup> that the cavitation nuclei are formed as a result of collisions of neutrons with nuclei of carbon (in the case of pentane) or oxygen (in the case of acetone), the recoil nuclei then interacting with the matter in accordance with Seitz's model.<sup>4</sup>

Sette *et al.*<sup>14,15</sup> found experimentally that the threshold amplitude of the ultrasonic field in water can be raised if the water is shielded by lead or paraffin. This suggested that the formation of the nucleating centers in the case of ultrasonic cavitation in water is connected with the cosmic-ray background. In these experiments, the cavitation was excited in water saturated with dissolved air at room temperature and was observed visually in a small region  $\sim 1$  cm<sup>3</sup>, where ultrasonic vibrations with frequency 1 MHz from a quartz emitter were focused. The threshold intensity<sup>1)</sup> of the ultrasonic field at this frequency was approximately equal to 1 W/cm<sup>2</sup>. One of the characteristic results obtained in Ref. 14 is shown in Fig. 4. Here, we have plotted the dependence of the threshold intensity  $W_{cr}$  of the ultrasonic field on the time of measurement when a lead shield 15-mm thick was used. As can be seen from the figure, after the introduction of the shield the cavitation strength begins to increase slowly to a value about 30% greater than the initial value. Removal of the shield leads to a gradual reduction of the cavitation strength to the original value. The introduction of a source of neutrons into a volume with water surrounded by a lead shield also leads to a gradual reduction of the cavitation strength to the original value. The characteristic time of variation of the cavitation strength is about 1000 sec. In contrast to the preceding experiments made with acetone and pentane, in which the lifetime of the nucleating bubbles was short, so that it was not possible to observe cavitation without the simultaneous application to the liquid of ionizing radiation and ultrasound, in the experiment with water the delayed effect of the shield and the source indicate that the cavitation nuclei arise here

<sup>1)</sup>The intensity  $W$  of an ultrasonic field is related to the pressure amplitude  $p_m$  in the ultrasonic wave by the equation  $W = p_m^2 / 2\rho c$ , where  $c$  is the velocity of sound in the medium.

without the acoustic field but grow to visible sizes only if an adequate acoustic field is applied. Analysis of the experimental data led Sette *et al.* to suggest that the occurrence of cavitation nuclei in the water is due to oxygen recoil nuclei formed by the interaction with fast neutrons ( $\sim 10$  MeV), or is due to the neutron source, or cosmic rays. Later, Sette *et al.*<sup>16</sup> showed that the introduction into distilled water of uranium salts lowers the threshold of ultrasonic cavitation by almost a factor of two.

In contrast to the investigations of Sette *et al.*, who used water with air dissolved in it, Finch<sup>17</sup> made similar experiments with degassed water. Cavitation was excited in a spherical 2-liter glass resonator by a 25-kHz ultrasonic field. The degassing of the water considerably raised the threshold amplitude  $p_{m,cr}$ —from 5–6 atm without a lead shield to 13 atm with a lead shield 10-mm thick. When the water was carefully degassed, its cavitation strength without a shield could be increased to 7–8 atm. When this water was irradiated with  $\sim 14$ -MeV neutrons,  $p_{m,cr}$  was reduced to below 5 atm (Fig. 5). The characteristic time of variation of the cavitation strength was of the order of several hours.

The influence of penetrating radiation on the cavitation strengths of a number of organic liquids was also investigated by Hahn.<sup>18</sup> He broke the liquids in a glass capillary with a constant stress produced by rapid rotation of the capillary around an axis perpendicular to its length. He found that the breaking strengths of the investigated liquids, which included Freon, isopentane, hexane, acetone, and others (altogether 28 liquids), was considerably reduced when they were exposed to  $\alpha$  particles, neutrons, and  $\gamma$  rays. A typical result of these measurements can be illustrated by the example of Freon, for which the cavitation threshold pressure was found to be  $p_{cr} \approx 5$  atm when irradiated with  $\alpha$  particles and neutrons and  $p_{cr} \approx 52$  atm with  $\gamma$  rays. In the absence of radioactive sources, it was found that  $p_{cr} \approx 120$  atm.

In the experiments described in Ref. 19 by Hahn *et al.*, the cavitation was excited by an ultrasonic field at 25 kHz in Freon and isopentane (in the presence of a neutron source) and also in methyl acetate (containing a dissolved uranium salt). Bubbles were observed in the Freon when the ultrasonic field had amplitude  $p_m = 5$  atm, and in the methyl acetate when  $p_m = 2$  atm. Detailed investigation of the development of the cavitation in the Freon showed that the bubbles are formed at the pressure crests of the standing ultrasonic waves. They grow to visible size ( $\sim 10^{-2}$  cm) during one period ( $\sim 10^{-5}$  sec), and disappear in a time corresponding to tens of

periods of the ultrasonic field. Acoustoluminescence was also observed in the form of short light pulses accompanying the formation of the cavities.

It should be noted that the experimental results obtained in Refs. 13–16 and 19 were not satisfactorily explained from the physical point of view. Above all, this applies to the experiments with water, in which the observed threshold amplitude  $p_{m,cr}$  was due to fairly large cavitation nuclei,  $\sim 10^{-4}$ – $10^{-3}$  cm. If the water is not degassed, such nucleating centers are always present.<sup>7</sup> Therefore, the suggestion of Refs. 13–17 that the cavitation nuclei are formed by fast neutrons ( $\sim 10$  MeV) through recoil nuclei interacting with the liquid in accordance with Seitz's mechanism<sup>4</sup> encounters a number of difficulties. Estimates show that such nuclei are incapable of depositing the energy (6) necessary for the formation of the cavitation nucleus in a path length  $10^{-3}$ – $10^{-4}$  cm. In this connection, it was suggested in Ref. 20 that small bubbles created by  $\delta$  electrons coalesce into a large bubble with a size rivaling that of the gas bubbles hitherto present in the water. Nor is it entirely clear how such bubbles can exist stably for many hours, as was observed in water.<sup>14</sup>

#### Attempts to make ultrasonic detectors of ionizing radiation

The experimental proof that ionizing radiation affects ultrasonic cavitation in liquids stimulated a search for ways to make fast particle detectors on the basis of this effect.

Hughes<sup>21</sup> attempted to make isopentane sensitive to a neutron flux by means of an ultrasonic field at frequency 31 kHz and amplitude  $\sim 2$  atm excited by a cylindrical radiator made of the piezoelectric ceramic barium titanate. Cavitation bubbles were observed in the liquid both in the presence of neutrons with energy from 10 to 23 MeV and in their absence. With the neutron source, cavitation arose within 10 msec; without it, only after 100 msec, though tracks were not observed.

Lyapidevskii *et al.*<sup>22</sup> investigated the influence of ultrasound on the lifetime of cavitation nuclei in a Freon bubble chamber irradiated with  $\gamma$  rays from a  $^{60}\text{Co}$  source. An ultrasonic field was excited by a magnetostrictive radiator at 25 kHz, although the ultrasound amplitude ( $\sim 5$  atm) was insufficient to make the liquid sensitive to the ionizing radiation.

Aleksandrov *et al.*<sup>23</sup> considered the possibility of making a propane chamber sensitive by excitation of sound with frequency from 50 to 500 Hz.

West<sup>24</sup> proposed and tested a neutron detector with degassed tetrachloroethylene. The liquid was made sensitive to ionizing radiation by an ultrasonic field excited by a cylindrical radiator in a glass resonator at frequency 21 kHz. It was assumed that cavitation bubbles can be detected by means of the shock wave pulses resulting from their collapse. Data were recorded by means of two microphones since the difference between the times of arrival of the sound signals at them could indicate the spatial position of the bubbles. In an ex-

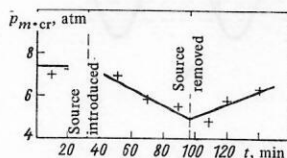


FIG. 5. Change in the threshold pressure of ultrasonic cavitation in water under the influence of 14-MeV neutrons.<sup>17</sup>



periment with a neutron source, it proved possible to record acoustic pulses that were repeated for many periods, indicating a continued existence of bubbles in the ultrasonic field.

In Refs. 25 and 26, it was suggested that the change in the thresholds of ultrasonic cavitation as a function of the intensity and energy of radiation could be used to determine very small neutron fluxes ( $E > 10$  MeV) or to detect in the liquids long-lived spontaneously fissile materials.

### Some conclusions from the experiments on the effect of ionizing radiation on ultrasonic cavitation

The experiments described above demonstrated convincingly that there is a connection of the ultrasonic cavitation phenomena in different liquids with ionizing radiation. As a rule, the experiments used liquids under far from critical conditions. Therefore, the available means for producing ultrasonic fields made it possible to stimulate growth to visible size of only comparatively large cavitation nuclei ( $\sim 10^{-4}$  cm) which, it was assumed, were formed directly in the liquid—by fission fragments—or indirectly—by fast neutrons ( $> 10$  MeV) through recoil nuclei. At the same time, analysis of the experimental data showed that fast charged particles (for example, protons) were incapable of forming bubbles of the necessary size at the available intensities of the ultrasonic field. Irradiation with positrons and  $\gamma$  rays also had no influence on the ultrasonic cavitation in the liquids.

The data on the cavitation strength of liquids exposed to  $\gamma$  rays give an idea about the amplitudes of the ultrasonic pressure needed to produce sensitivity to particles with minimal ionization. For example, the cavitation strength of Freon at atmospheric pressure when exposed to electrons formed by  $\gamma$  rays is about 50 atm. It would be rather difficult to produce an ultrasonic field of this pressure amplitude in a significant volume of liquid by means of the currently known ultrasonic systems. Therefore, none of the attempts to make an ultrasonic track detector of fast particles was successful.

In order to solve the problem of detecting particles with minimal ionization in an ultrasonic field, all the subsequent investigations described below were made under the following conditions:

First, attention was concentrated on cryogenic liquids, which are free of impurity-induced cavitation nuclei. The main aim was to make liquid hydrogen sensitive to ionizing radiation. At the same time, some attention was devoted to liquid helium, a medium capable of being sensitive to ionizing radiation at small superheatings.

Second, to ensure the formation of bubbles with small cavitation nuclei the working temperature of the liquids was taken in the region of normal operation of an ordinary bubble chamber.

Third, the possibility was considered of the cavitation nuclei growing to visible size during many periods of the ultrasonic field.

## 2. EXPERIMENTAL JUSTIFICATION OF THE POSSIBILITY OF MAKING USBCs

### Principle of operation of USBCs

An idea of the formation of tracks of ionizing particles in an USBC can be obtained in Fig. 6, which shows the pressure distribution in the field of a plane standing ultrasonic wave. At the times corresponding to the maximal pressure at the crests of the standing wave, the pressure distribution in space corresponds to the continuous curve in Fig. 6a ( $p_s$  is the pressure of the threshold sensitivity of the chamber, and all the other notation has already been introduced). It is obvious that in the regions in which the pressure in the liquid is lower than  $p_s$  one can expect sensitivity of the liquid to ionizing radiation. At each given time, the track of a particle will consist of spatially periodic groups of bubbles separated by the wavelength  $\lambda$ . At the same time, neighboring regions separated by  $\lambda/2$  from the sensitivity regions are insensitive to the ionizing radiation. After a time  $1/2f$ , where  $f$  is the frequency of the ultrasonic field, the pressure distribution corresponds to the dashed curve in Fig. 6a, and in these regions tracks can be detected. Thus, the groups of bubbles that form the tracks of two particles that enter the chamber in succession separated by a time interval  $1/2f$  will be displaced in space with respect to one another by  $\lambda/2$ .

The distribution of the pressure in time in a region corresponding to a crest of the standing wave is shown in Fig. 6b. A particle that passes through this region during the time interval  $\Delta t = t_2 - t_1$  can form bubbles of critical radius along its path. Thus, the fraction of time during which the USBC is sensitive to the ionizing radiation is  $2 \Delta t f$ .

Depending on the amplitude  $p_m$  of the ultrasonic field, one can have two regimes of operation in an USBC. At amplitudes  $p_m$  that slightly exceed the threshold pressure  $p_{m,cr}$ , the so-called many-period regime is realized. In this case, pulsed ultrasonic vibrations, i.e., trains of tens of vibrations, are applied to the working medium of the chamber. A critical cavitation nucleus formed in a negative half-period does not succeed in collapsing completely but is merely reduced to a certain size. Subsequently, the bubble grows to visible size over several periods of the ultrasonic field. The physical picture of such growth of the cavitation nuclei will be con-

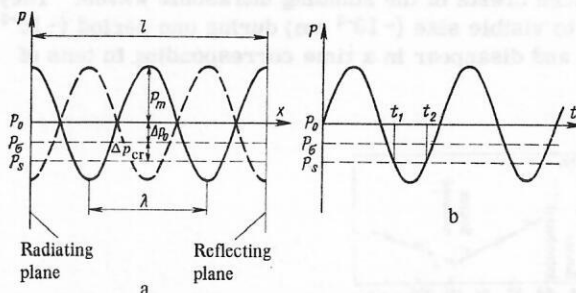


FIG. 6. Distribution of pressure in space (a) and in time (b) in the field of a standing ultrasonic wave.

sidered in detail below. When the ultrasonic field is removed, the bubble collapses completely at a rate determined by the excess static pressure  $\Delta p_0$ . A different, single-period regime of operation of an USBC can be achieved at amplitudes  $p_m$  of the ultrasonic field appreciably exceeding  $p_{m,cr}$ ; this is hard to achieve in many liquids. In this case, the bubble must grow to visible size during the negative half-period of the ultrasonic wave and collapse in the positive half-period following it. Realization of such a regime would make it possible to construct an USBC with high repetition rate.

### Generation of strong ultrasonic fields

We give some relations and characteristics relating to ultrasonic transducers and the fields they produce.<sup>27,28</sup> A transducer which is operating under a regime in which ultrasonic energy is radiated into a surrounding medium may be called an ultrasonic radiator.

An important characteristic of an ultrasonic radiator is the coefficient of electromechanical coupling, which characterizes the ratio of its mechanical energy to the supplied electrical energy. The piezoelectric ceramic materials barium titanate and lead zirconate-titanate (PZT) have the highest coefficients of electromechanical coupling. They are the most effective for making ultrasonic emitters for USBCs.

Another characteristic of the radiator is the electroacoustic efficiency  $\eta_{e,a}$ , which determines the ratio of the emitted acoustic energy to the supplied electrical energy. It can be represented as  $\eta_{e,a} = \eta_{e,m} \eta_{m,a}$ , where  $\eta_{e,m}$  is the electromechanical efficiency and  $\eta_{m,a}$  is the mechanicoacoustical efficiency. The electromechanical efficiency for a piezoceramic is near unity since the dielectric losses in it are small. Therefore, the efficiency of a piezoelectric transducer is largely determined by the mechanical losses in the active material and the constructional elements during the mechanicoacoustical transformation of the energy, i.e., it is determined by the mechanicoacoustical efficiency.

When a radiator is excited, its surface is affected by the reaction of the working medium. If the emitting surface is wider than the wavelength of the acoustic wave in the surrounding medium, the input impedance  $Z$  on the surface of the radiator (the resistance of the radiation) can be regarded as a purely active quality, and in the case of traveling waves  $Z = \rho c S$  ( $S$  is the area of the emitting surface). For effective emission of acoustic energy, the radiator must be optimally matched to the medium. Otherwise, when the voltage  $V$  is raised, mechanical fracture of the radiator occurs before the necessary amplitude of the acoustic pressure is reached. In order to raise the input impedance on the surface of the radiator in an USBC, ultrasonic systems consisting of two planar radiators are usually used. The distance  $l$  between the radiators must be an integral multiple of the ultrasound wavelength in the medium. In this case, a field of plane standing waves is formed, and the input impedance of each radiator can be expressed in the form  $Z = 2\rho c S / \alpha l$ , where  $\alpha$  is the coefficient of absorption of sound in the medium. This expression for  $Z$  is valid

for small values of  $\alpha$ , when  $\alpha l \ll 1$ , which is usually satisfied in USBCs at ultrasonic frequencies of the order of tens of kilohertz. In such ultrasonic systems, a flat reflecting wall can be used instead of one of the radiators.

Depending on the type of working liquid and the thermodynamic conditions in the USBC, the generation of a strong ultrasonic field has particular problems in each concrete case. The parameters of the ultrasonic field needed to make various liquids sensitive to ionizing radiation are given in Table I. Let us consider the ultrasonic emitting systems that can be used in USBCs.

*Simple resonant piezoceramic elements.* They can be successfully used in media in which comparatively low ultrasound intensities are needed to make the liquids sensitive. It can be seen from Table I that liquid helium is such a medium. Therefore, in liquid helium it proved comparatively easy to obtain tracks of ionizing particles<sup>29-31</sup> using simple resonant piezoceramic elements as ultrasonic radiators. The ultrasonic system used in these investigations consisted of two piezoceramic disks that produced a field of plane standing waves. The parameters of this system and the ultrasonic field are given in Table II.

*Reinforced composite radiators.* It is a very complicated problem to radiate ultrasonic energy into liquid hydrogen.<sup>32</sup> It can be seen from Table I that this requires large pressure amplitudes and high intensity of the ultrasound combined with a low acoustic resistance  $\rho c$  of the medium.

In Refs. 33 and 34 it was shown that the use in liquid hydrogen USBCs of simple piezoceramic elements, even when made in the form of binary systems, does not enable one to achieve the desired effect—the piezoelements break before the ultrasound intensity needed for the formation of tracks is reached in the liquid hydrogen.

The ceramic can be reinforced however. The constructions of composite reinforced radiators specially developed for use in cryogenic liquids<sup>33,35</sup> are shown in Fig. 7. Their construction took into account the experience gained from developing reinforced ultrasonic radiators intended for ordinary liquids.<sup>36</sup> As can be seen from Fig. 7, the piezoceramic elements are placed between metallic plates, which makes it possible to produce a static compression by means of a reinforcing nut. On assembly, the piezoelements were compressed to  $\sim 200 \text{ kg/cm}^2$ , which appreciably increased the mechanical strength of the radiators. If the metallic elements used in the construction have a coefficient of thermal expansion nearly equal to the piezoceramic's (for example, titanium alloys), the static compression can be preserved at low temperatures. To ensure acoustic contact, indium washers were placed between the piezoceramic and the metal. As can be seen in Fig. 7, the emitting surface of the transducer is larger than that of the piezoelectric elements. This construction is chosen to raise the input impedance. In addition, the active elements themselves are taken out of the central zone, where the deformations and internal losses are maximal.<sup>37</sup> All these measures together increase the acous-



tomechanical efficiency, which is close to 0.35 according to measurements made under traveling wave conditions in liquid hydrogen. At a resonance frequency 38.4

kHz and voltage 1.5 kV it was possible, using such radiators, to produce an ultrasonic field in liquid hydrogen with amplitude  $\sim 3$  atm (Ref. 35).

TABLE II. Experiments on the influence of an ultrasonic field on the formation of tracks of ionizing particles in bubble chambers.

Regime of operation of chamber	Working liquid in chamber	Particles, source (energy or momentum)	Thermodynamic conditions					Time characteristics					
			$T_0$ , °K	$p_0'$ atm	$p_0$ atm	$p_\sigma$ atm	$\Delta p_0$ atm	$\tau_1$ , msec	$\tau_2$ , msec	$\Delta t_1$ , msec	$\Delta t_2$ , msec	$\Delta t_3$ , msec	
Combined effect of expansion system and ultrasonic field	Hydrogen	$\gamma$ rays, $^{60}\text{Co}$ source	27	5.8	3.4	4.8	$(-1.4)$	10	15	—	2-2.5	—	
		$\pi^-$ mesons (340 MeV)								5-10		0.3	
	Hydrogen	$\gamma$ rays, pulsed $^{60}\text{Co}$ source	24.9	3.9	1.4-2.5	3.2	$(-0.7)-(-2.1)$	40	1-5		0.5-10	1	
			26.9	5.2	2-5.2	4.8	$(-2.8)-(+0.4)$						
	Hydrogen	$\pi^-$ mesons (340 MeV)	27	5.2	4.5-4.8	4.8	$(-0.3)-0$	10	10	5	2	0.3	
Effect of ultrasonic field alone (USBC regime)	Helium	$\pi$ mesons and protons	3.4-3.65	—	0.4-0.6	0.4-0.6	0	—				0.6-2	
		(1 GeV/c)	3.25	—	0.6	0.35	0.25	—	1			0.6-2	
			3.25	—	0.4	0.35	0.08	—	3			0.6-2	
	Hydrogen	$\pi^-$ mesons (340 MeV)	27	—	5.15	4.8	0.35	—	4.5	1-4	1.5-2.5	0.3	
	Hydrogen	$\gamma$ rays, $^{60}\text{Co}$ source	21-28	—		1.2-5.8	0.15-0.4	—	1-2.5	—	0.2-1.0	—	
	Hydrogen	$\gamma$ rays, $^{60}\text{Co}$ source	24-26	—		2.6-4.0	0.2-0.4	—	10	—		—	
		Electrons (300 MeV)											
Regime of operation of chamber	Working liquid in chamber	Particles, source (energy or momentum)	Parameters of ultrasonic systems								Institute, literature		
			Type of system, piezoceramic		Diameter of radiator, mm		Working region, mm( $\lambda$ )		$f$ , kHz $V$ , kV			$p_m$ , atm	
Combined effect of expansion system and ultrasonic field	Hydrogen	$\gamma$ rays, $^{60}\text{Co}$ source	Cylindrical focusing system (barium titanate)		External $\varnothing$ 115, internal $\varnothing$ 70, height 60		$\varnothing$ 70 ( $\sim \lambda$ )		14   1.2		$\sim 1.0$		JINR, Acoustics Institute (Ref. 32)
		$\pi^-$ mesons (340 MeV)											
		Hydrogen	$\gamma$ rays, pulsed $^{60}\text{Co}$ source	System of simple planar pairs of radiators (PZT-4)		$\varnothing$ 50, thickness 6		60 (25 $\lambda$ )		360   0.9		0.9	
	Hydrogen	$\pi^-$ mesons (340 MeV)	System of planar composite reinforced pairs of radiators (PZT-23)		$\varnothing$ 50		58 (2 $\lambda$ )		30   1.2		1.75		JINR, Acoustics Institute (Ref. 33)
Effect of ultrasonic field alone (USBC regime)	Helium	$\pi$ mesons and protons 1(GeV/c)	System of simple planar pairs of radiators (PZT-4)		$\varnothing$ 70		50		110   0.7		$>0.45$		CERN (Ref. 29)
					$\varnothing$ 70		40		97   0.7		$>0.35$		CERN (Ref. 30)
					$\varnothing$ 70		40		97   1.0		$>0.21$		CERN (Ref. 30)
	Hydrogen	$\pi^-$ mesons (340 MeV)	System of planar composite reinforced pairs of radiators (PZT-23)		$\varnothing$ 70		90 (4 $\lambda$ )		38.4   1.5		$\sim 3.0$		JINR, Acoustics Institute (Ref. 35)
	Hydrogen	$\gamma$ rays, $^{60}\text{Co}$ source	System of planar pairs of radiators with matching plate (PZT-4)		$\varnothing$ 70		60 (20 $\lambda$ )		300   1.2		$>2.8$		CERN (Ref. 33)
	Hydrogen	$\gamma$ rays, $^{60}\text{Co}$ source	System of planar radiator with reflector (NEPEC)		$\varnothing$ 40, thickness 6		28 (10 $\lambda$ )		340   1-1.6		1-1.6		Tokyo University (Ref. 41)
Electrons (300 MeV)													

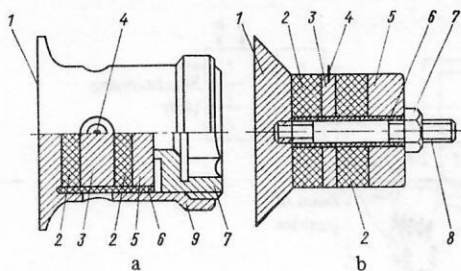


FIG. 7. Composite reinforced ultrasonic radiators for liquid hydrogen (Refs. 33 and 35). a) Radiator reinforced in a jacket; b) radiator reinforced on a rod; 1) radiating surface; 2) piezo-ceramic disks; 3) and 5) metallic disks; 4) terminal; 6) teflon insulator; 7) reinforcing nut; 8) reinforcing rod; 9) jacket.

**Composite radiators with matching plates.** During operation at high frequencies, radiator pairs can break as a result of mismatch of the resonance cavity resulting from a change in the temperature of the liquid or the development of cavitation phenomena on the surface of the radiators, which change the velocity of sound. For example, in the case of liquid hydrogen, ultrasound of frequency 300 kHz, and a resonance cavity of length  $25\lambda$ , mismatch of the cavity by  $\lambda/4$  can be caused by a change in the velocity of sound by only 1%, which can occur if the temperature changes by  $0.1^\circ\text{K}$  (Ref. 38). Then on the surface of the emitter there is a pressure node and not a pressure crest, and the effective input impedance is drastically reduced. In order to match better the impedances of the liquid and the piezoceramic, one can introduce between them a quarter-wave plate with characteristic impedance  $(\rho c)_{p1}$  intermediate between those of the piezoceramic and the working medium. Two types of radiators containing a quarter-wave matching plate are shown in Fig. 8. These radiators made it possible to obtain a pressure amplitude  $\sim 2.8$  atm in liquid hydrogen at a frequency 300 kHz (Ref. 39).

**Focusing ultrasonic systems.** Obviously, if focusing

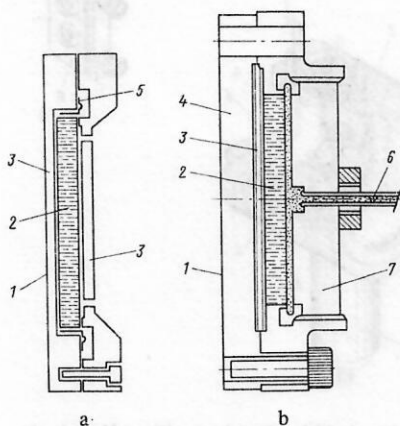


FIG. 8. Radiators with matching plates for liquid hydrogen (Ref. 39). a) System with glued disks (the glue a mixture of isopentane and trimethylbutane); b) radiators with disks pressurized by helium gas at 50 atm; 1) radiating surface; 2) piezoceramic disk; 3)  $\lambda/4$  perspex matching plate; 4) aluminum disk  $\lambda/2$  thick; 5) mylar ring seal glued by araldite; 6) tube for gaseous helium; 7) steel disk  $3\lambda/4$  thick.

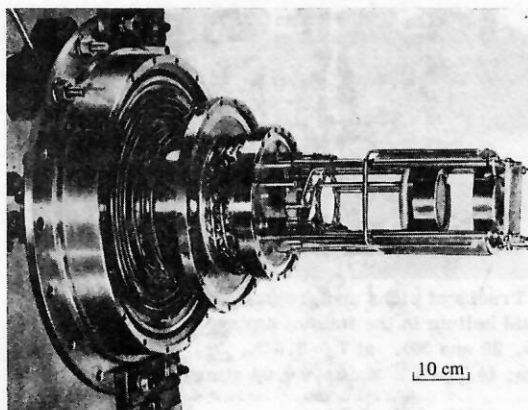


FIG. 9. System of ultrasonic radiators for helium USBC.<sup>29</sup>

systems are used, one can obtain fairly high ultrasound intensities in a certain region of the working volume of an USBC. At the same time, only small electric voltages need be applied to the piezoceramic.

In Ref. 32, a radiator made of piezoceramic sections of barium titanate forming an annular layer was used. This was tightened by a metallic ring hot-fitted onto the cylinder. The internal diameter of the radiator was 7 cm. This radiator, working at the resonance frequency 14 kHz and voltage  $V \approx 1.2$  kV, produced a pressure  $p_m \approx 1$  atm in an appreciable part of the volume enclosed within the cylinder.

#### Helium USBC. Use of planar emitters

The first tracks of particles with minimum ionization were detected in the helium USBC made at CERN.<sup>29</sup>

The chamber was a glass cylinder containing two PZT-4 radiators of diameter 7 cm. The distance  $l$  between them was varied from 5 to 25 cm by means of an external mechanical device. The general form of the ultrasonic system is shown in Fig. 9. In this experiment, the distance  $l$  was equal to 5 cm, which corresponded to 25 wavelengths of the ultrasonic waves excited in the liquid by the radiators at the resonance frequency 110 kHz. The chamber operated in the temperature range from 3.4 to  $3.65^\circ\text{K}$  at a pressure corresponding to the saturated vapor pressure, i.e., with  $\Delta p_0 = 0$ . Under these conditions, it proved possible to obtain tracks of pions and protons with minimum ionization. The bubbles in the tracks grew to a visible size ( $\sim 10^{-2}$  cm) during 0.6 msec, which corresponded to 50–60 cycles of the ultrasonic field. The density of bubbles along the tracks was  $8\text{--}10\text{ cm}^{-1}$ . Comparison of the number of observed tracks with the intensity of the particle beam showed that the chamber was sensitive for 50% of the time. According to estimates, the amplitude of the ultrasonic pressure was not less than 0.45 atm.

In other experiments<sup>30</sup> made under conditions when an excess pressure was produced in the working volume of the chamber of magnitude  $\Delta p_0 \approx 0.2$  atm, which prevents spontaneous boiling of the liquid, it was possible to estimate the practically achievable repetition rate of the helium USBC ( $\sim 100$  cycle/sec).



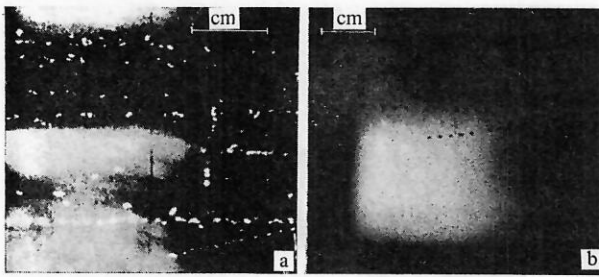


FIG. 10. Tracks of pions and protons with minimum ionization in liquid helium in the field of a plane standing ultrasonic wave (Refs. 29 and 39). a)  $T_0 = 3.5^\circ\text{K}$ ,  $\Delta p_0 \approx 0$ ,  $f = 110\text{ kHz}$ ,  $\lambda \approx 0.15\text{ cm}$ ; b)  $T_0 = 3.2^\circ\text{K}$ ,  $\Delta p_0 = 0.04\text{ atm}$ ,  $f = 100\text{ kHz}$ ,  $\lambda \approx 0.2\text{ cm}$ .

The tracks of high energy particles (beam of pions and protons with momentum  $1\text{ GeV}/c$ ) obtained in the helium USBC are shown in Fig. 10. The conditions under which the experiments were made are given in Table II.

### Liquid hydrogen USBC. Use of focusing ultrasonic systems and planar radiators

Because of the difficulties mentioned above of obtaining strong ultrasonic fields in liquid hydrogen, the first experiments<sup>32-34</sup> aimed at making this liquid sensitive to ionizing radiation were made in ordinary liquid-hydrogen bubble chambers, in which, in addition to the excitation of ultrasonic vibrations, the working medium was superheated to a certain extent by a mechanical expansion system. Figure 11 shows the variation of the pressure in the chamber with the experiment arranged in this way. It can be seen from Fig. 11 that the pressure  $p_0$

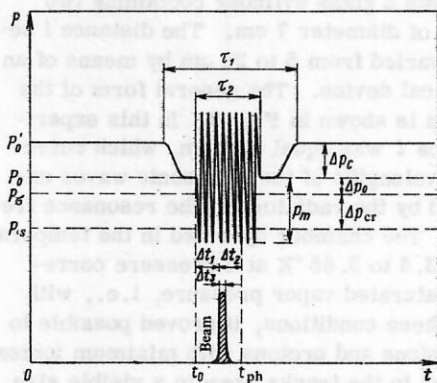


FIG. 11. Diagram of variation of the pressure with time in the working volume of a bubble chamber with combined influence of ultrasound and a mechanical expansion system.  $p'_0$  is the original static pressure;  $p_0$ , the saturated vapor pressure;  $p_0$ , the static pressure produced by the expansion system;  $p_s$  is the threshold sensitivity pressure;  $p_m$  is the pressure amplitude of the ultrasonic field;  $\Delta p_0$  is the static excess pressure;  $\Delta p_{cr}$  is the cavitation threshold;  $\Delta p_c$  is the change in the pressure produced by the expansion system;  $\tau_1$  is the duration of the mechanical expansion pulse;  $\tau_2$  is the duration of the ultrasound pulse;  $\Delta t_1$  is the time lag of the particle beam after the start of the ultrasonic pulse;  $\Delta t_2$  is the time delay of photographing after the introduction of the particle beam (the growth time of the bubbles);  $\Delta t_3$  is the pulse duration of the particle beam;  $t_0$  is the start of the ultrasonic pulse;  $t_{ph}$  is the start of photographing.

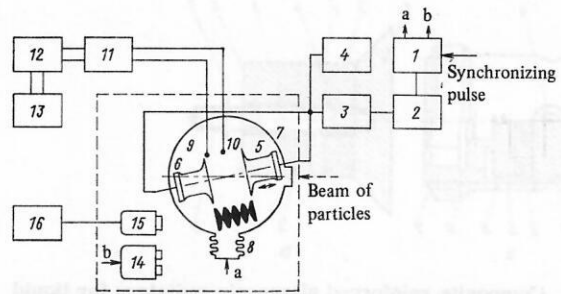


FIG. 12. Block diagram of experimental apparatus for investigating the influence of ultrasound on the formation of tracks of ionizing particles in a liquid hydrogen bubble chamber (Ref. 33). 1 is the synchronizing block; 2 is the supplying generator for the series of vibrations; 3 is a power amplifier; 4 is a pulse voltmeter; 5 and 6 are ultrasonic radiators; 7 is the liquid hydrogen bubble chamber; 8 is the mechanical expansion system; 9 and 10 are miniature ultrasonic receivers; 11 are amplifiers; 12 is an oscillograph; 13 is a voltmeter; 14 is a stereographic camera; 15 is a transmitting telecamera; 16 is a receiving telecamera.

acting constantly on the liquid (see Fig. 6) under an USBC regime was produced in this case for only a short period when the ultrasonic pulse was applied. The value of  $p_0$  was varied during the experiment by choosing the amount of expansion of the working volume of the chamber and could reach the original static pressure  $p'_0$ . When pulsed particle beams were used, the passage of the particles through the working volume of the chamber could be rigorously synchronized with the switching on of the mechanical expansion system, the introduction of the ultrasonic pulse into the liquid, and the time of photographing. A block diagram of the apparatus used in one of these experiments<sup>33</sup> is shown in Fig. 12.

The first combined system including an expansion

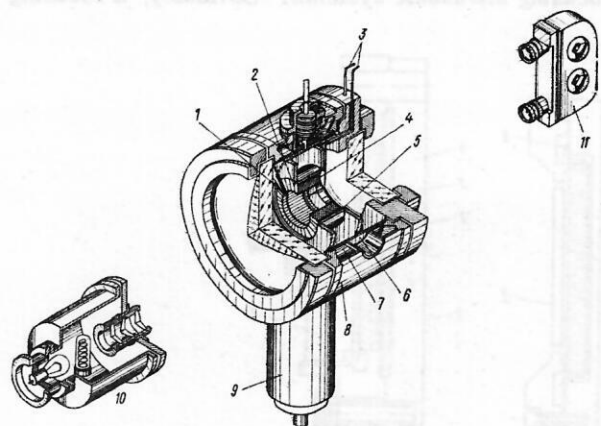


FIG. 13. Liquid hydrogen bubble chamber with cylindrical focusing ultrasonic radiator (Ref. 32). 1 is a miniature ultrasonic receiver; 2 is a cylindrical focusing ultrasonic radiator; 3 is the current input; 4 is a layer of the radiator; 5 is a reinforced hoop; 6 is a window for introducing the particle beam; 7 is a temperature control jacket; 8 is the frame of the chamber; 9 is the mechanical expansion system; 10 is an illuminator; 11 is a stereographic camera.

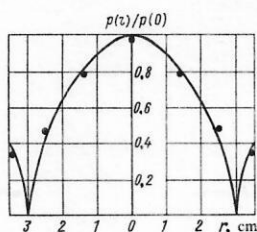


FIG. 14. Radial distribution of the ultrasonic pressure in a cylindrical focusing radiator (Ref. 32).  $p(r)/p(0)$  is the ratio of the pressure at the point with coordinate  $r$  to the maximal pressure on the cylinder axis.

system and ultrasonic radiators was used in Ref. 32 in a collaboration between the Joint Institute for Nuclear Research and the Acoustics Institute. The experiment used a 25-cm liquid hydrogen bubble chamber,<sup>40</sup> in whose working volume a cylindrical focusing radiator (Fig. 13) working at resonance frequency 14 kHz was placed. The radial distribution of the acoustic pressure produced by this radiator in carbon tetrachloride, in which the velocity of sound is close to the velocity of sound in liquid hydrogen at  $T_0 = 27^\circ\text{K}$ , is shown in Fig. 14. The tracks of ionizing particles were formed either by  $\gamma$  rays from the radioactive source  $^{60}\text{Co}$  or by a beam of 340-MeV  $\pi^-$  mesons from the Dubna synchrocyclotron. The duration  $\tau_2$  of the ultrasonic pulse applied to the radiator was 15 msec and was somewhat longer than the duration  $\tau_1$  of the chamber expansion pulse, which was equal to 10 msec. Tracks of negative pions obtained in this experiment with mechanical expansion corresponding to the minimal sensitivity of the chamber are shown in Fig. 15.

The results of this experiment demonstrated the basic possibility of complete replacement of the expansion system of a liquid hydrogen bubble chamber by an ultrasonic vibratory system. Therefore, in subsequent experiments, measures were undertaken to improve considerably the parameters of the ultrasonic systems with the aim of dispensing gradually with the expansion sys-

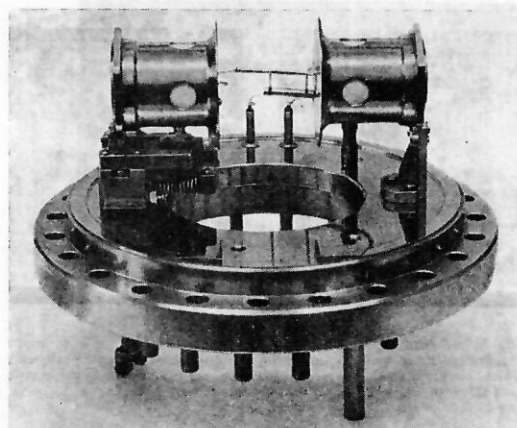


FIG. 16. System of ultrasonic radiators for liquid hydrogen USBC.<sup>33</sup>

tem. Considerable attention was devoted to restricting parasitic boiling (cavitation) on the surface of the radiators (the light halo in Fig. 15b). It was found that shortening the duration of the ultrasonic pulses, the use of radiators with high efficiency, and careful polishing of the emitting surfaces considerably reduced the effect of cavitation phenomena.

In Ref. 33, a pair of planar reinforced composite radiators (see Fig. 7a) working at the resonance frequency  $f \approx 30$  kHz was used to produce standing waves of comparatively large amplitudes in liquid hydrogen and tracks of 340-MeV  $\pi^-$  mesons were obtained in a 25-cm liquid hydrogen bubble chamber at a static pressure corresponding to the saturated vapor pressure. The general form of the ultrasonic instrument used in this experiment is shown in Fig. 16. During the experiment, the static excess pressure  $\Delta p_0$  was varied from  $-0.3$  atm to 0 by means of a mechanical expansion system; the time interval between the photographing and the introduction of the beam of particles was about 2 msec, which corresponded to 60 periods of the ultrasonic field. With voltage  $V = 1$  kV on the radiators, the pressure amplitude  $p_m$  reached  $\sim 1.5$  atm. Photographs of tracks obtained at different values of  $\Delta p_0$  and  $V$  are reproduced in Fig. 17.

Experimental data on the formation of tracks of charged particles in a liquid hydrogen bubble chamber with simultaneous use of expansion and ultrasonic systems were also obtained in the investigation Ref. 34 made at CERN. The experiments were made on the meter model of the Large European Bubble Chamber in whose working volume two simple PZT-4 radiators were placed.

Further improvement of the ultrasonic systems made it possible to dispense completely with the mechanical expansion system in the liquid hydrogen bubble chambers. In the experiments of Ref. 39, which were made at CERN in a wide range of temperatures ( $21$ – $28^\circ\text{K}$ ) using only an ultrasonic field (300 kHz) produced by radiators with matching plates, it was demonstrated that liquid hydrogen is sensitive to Compton electrons from

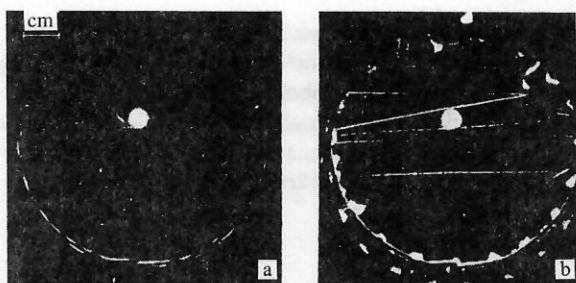


FIG. 15. Tracks of negative 340-MeV pions in a liquid hydrogen bubble chamber under the combined influence of ultrasound and mechanical expansion corresponding to minimal sensitivity of the chamber<sup>32</sup> at  $T_0 = 27^\circ\text{K}$ ,  $f = 14$  kHz,  $V = 1.2$  kV,  $\tau_1 = 10$  msec, and  $\tau_2 = 15$  msec. a) Without ultrasound; b) with ultrasound.



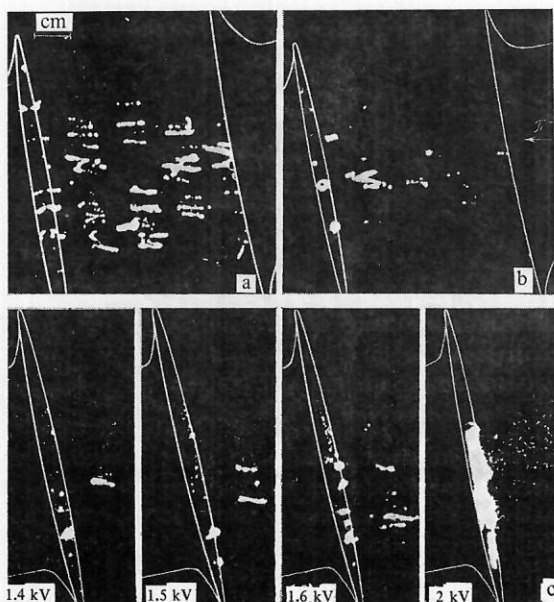


FIG. 17. Tracks of negative 340-MeV pions in liquid hydrogen bubble chamber under the influence of plane standing ultrasonic wave<sup>33</sup> at  $T_0=27^\circ\text{K}$  ( $p_0=4.8$  atm),  $p'_0=5.2$  atm,  $f=30$  kHz,  $\tau_2=10$  msec,  $\Delta t_1=5$  msec,  $\Delta t_2=2$  msec. a)  $p_0=4.5$  atm,  $\Delta p_0=-0.3$  atm,  $V=1.0$  kV; b)  $p_0=4.65$  atm,  $\Delta p_0=-0.15$  atm,  $V=1.0$  kV; c)  $p_0=4.8$  atm,  $\Delta p_0=0$  (at different voltages).

$\gamma$  rays of a  $^{60}\text{Co}$  source at  $\Delta p_0=0.15-0.4$  atm (Fig. 18). In the experiment of Ref. 35, made at Dubna and also in liquid hydrogen with  $\Delta p_0=0.35$  atm by means of only an ultrasonic field (38.4 kHz) produced by reinforced radiators (see Fig. 7b), tracks of 340-MeV  $\pi^-$  mesons were obtained (Fig. 19). Experiments made later at Tokyo University<sup>41</sup> showed that Compton electrons from  $^{60}\text{Co}$   $\gamma$  rays readily form cavitation bubbles in liquid hydrogen under the influence of an ultrasonic field of frequency 300 kHz produced by an isolated piezoceramic disk that emits acoustic energy in the direction of a reflecting wall. In the same experiments, when the liquid hydrogen was irradiated with 300-MeV electrons, poorly distinguishable tracks were observed on the background of the irregularly formed bubbles of parasitic boiling.

A complete list of all the experiments designed to make liquid hydrogen ultrasonically sensitive to ionizing radiation is given in Table II.



FIG. 18. Tracks of Compton electrons in liquid hydrogen USBC with field of a plane standing ultrasonic wave of frequency 300 kHz (Ref. 39) at  $T_0=24.6^\circ\text{K}$ ,  $\Delta p_0=0.4$  atm,  $V=1.5$  kV,  $\tau_2=2.5$  msec.

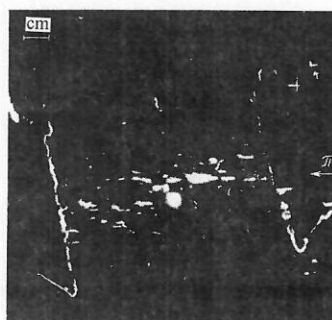


FIG. 19. Tracks of negative 340-MeV pions in liquid hydrogen USBC in a field of a plane standing ultrasonic wave of frequency 38.4 kHz (Ref. 35) at  $T_0=27^\circ\text{K}$ ,  $\Delta p_0=0.35$  atm,  $V=1.5$  kV,  $\tau_2=4.5$  msec,  $\Delta t_2=2$  msec.

### The most important experimental results from the investigation of the operation of USBCs

*Pressure amplitude in ultrasonic waves and factors that restrict it.* As the experiments showed, the pressure amplitude  $p_m$  of the ultrasonic field is restricted primarily by cavitation phenomena on the surface of the radiators. When cavitation occurs, the input impedance on the surface of the radiators is reduced<sup>42</sup> because the density of the medium and the velocity of sound in it decrease.<sup>43</sup> As a consequence, the efficiency of the radiators is reduced and so is the pressure amplitude  $p_m$  of the ultrasonic field. The change in the velocity of sound also leads to a mismatch of the resonance length  $l$  (see Fig. 6), resulting in a violation of the condition of multiplicity of the wavelength  $\lambda$ . As a result, the field of standing waves in the working volume of the USBC is "broken up."

There is no doubt also that, in the absence of cavitation, the absorption of ultrasound in the medium due to viscous loss, relaxation loss, and the expenditure of energy on the growth of the vapor bubbles that form the tracks also reduces the pressure amplitude. However, as estimates made<sup>35,42</sup> for liquid hydrogen at frequencies of the order of tens of kilohertz show, the influence of these factors is insignificant for the concentrations of vapor bubbles in the working volume of the USBCs and the sizes of the instruments that have been used in experiments.

Direct measurements show that at a given  $\Delta p_0$  a linear dependence of the pressure amplitude on the voltage applied to the radiators is observed only up to certain voltages. The dependence measured in liquid hydrogen by means of a miniature acoustic receiver at a pressure crest<sup>33</sup> is shown in Fig. 20, from which it can be seen

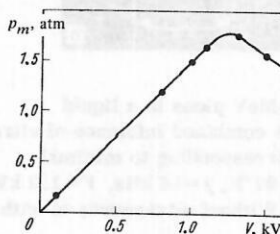


FIG. 20. Dependence of the pressure amplitude  $p_m$  of ultrasonic field on the voltage  $V$  applied to the ultrasonic radiators.<sup>33</sup>

that when cavitation occurs the amplitude of the ultrasonic field reaches saturation and then begins to decrease. The same effect was noted in Ref. 30, in which the amplitude  $p_m$  was measured by means of one of a pair of planar radiators that was operating as a receiver of ultrasound.

Measurements of the sizes of the bubbles forming the tracks and the bubbles on the radiator surfaces at different voltages for the case of liquid hydrogen<sup>33</sup> show that when the voltage is increased the track bubbles grow only to a definite limit, whereas the parasitic-boiling bubbles continue to increase. At high voltages, the tracks are completely suppressed and the cavitation on the emitter surface becomes predominant (see Fig. 17c at  $V = 2.0$  kV).

It should be noted that exact measurement of the pressure amplitude of the ultrasonic field in the case of cavitation is a rather difficult problem. Thus, if ultrasound receivers are used, complications arise because of cavitation on their surfaces. Therefore, in many cases the data given are not very accurate and they are sometimes deduced indirectly. In Refs. 34 and 39, the amplitude of the ultrasound pressure was estimated by measuring the density of bubbles along the tracks of particles under the assumption that the density of bubbles depends on the expansion pressure and the temperature in the USBC in the same way as in an ordinary bubble chamber.

*Growth time and size of bubbles in USBCs.* The available data on the rate of growth and sizes of bubbles in USBC are rather approximate since they were obtained under conditions that precluded an examination of the behavior in time of the bubbles in the ultrasonic field. The data refer only to comparatively large bubbles ( $\sim 10^{-2}$  cm) that can be photographed by means of the optical systems used in ordinary bubble chambers. Considerable uncertainties are due to the impossibility of exact determination of the time of formation of the cavitation nuclei. Some experiments were made under conditions when the USBC was irradiated with a constant source of  $\gamma$  rays, for which a statistical distribution of the intensity in time is characteristic. Even when an USBC is used in accelerator beams or in a beam from a pulsed source of  $\gamma$  rays, when one can synchronize the start of the ultrasound pulse, the particle beam, and the time of photographing, a large spread of bubble sizes is observed. It can be explained by the following factors: First, because of the long duration of the beam pulses employed, which appreciably exceed the period of the ultrasonic field, the cavitation nuclei may begin their growth at different phases of the ultrasonic pressure; second, because the duration of the particle beams is comparable with the time interval between the start of the beam pulse and the time of photographing, the time of growth for bubbles produced by individual particles may be different.

In all experimental investigations it has been noted that in an ultrasonic field the bubbles grow very rapidly to a visible size. However, because of the uncertainties discussed above, it is difficult to establish a lower limit of their growth time. As follows from the experiment

with the helium USBC,<sup>29</sup> visible bubbles ( $\sim 10^{-2}$  cm) are observed even at an ultrasonic pulse duration of  $\sim 0.6$  msec (which corresponds to 50–60 periods at frequency 110 kHz). If, in addition, one takes into account the time required to establish the ultrasonic field between the radiators, the growth time may be shorter than 0.6 msec. A rapid rate of growth of bubbles in liquid hydrogen USBCs is also indicated. In Ref. 39, in which an ultrasonic field of frequency 300 kHz was used, it was noted that less than 1 msec is required to obtain bubbles with diameter 0.1 cm. In Ref. 35, bubbles of diameter 0.02–0.1 cm were obtained with ultrasound of 38.4 kHz in a time of  $\sim 2$  msec, which corresponded to 80 periods of the ultrasonic field.

In the last case it was characteristic that, besides small bubbles, an appreciable number of large bubbles was observed, these being formed apparently over a longer period of time. The appearance of the large bubbles can be attributed to the features of their growth in the ultrasonic field.<sup>44</sup> In experiments in which a combination of mechanical and ultrasonic systems was used,<sup>34</sup> it was noted that once  $\Delta p_c + p_m$  exceeds the level of sensitivity and the time delays of the light pulse  $\Delta t_2$  are greater than 1 msec, the bubbles obtained in the ultrasonic field have diameters five times greater than the bubbles formed when only the expansion system is used. It was also noted that there is a qualitative difference between the bubbles formed by the ordinary expansion system and by ultrasound in conjunction with the expansion system. The former appear as transparent spheres, while the latter, when their diameter exceeds 0.02 cm, are opaque clusters of many bubbles. The occurrence of such clusters was also noted in other investigations.<sup>29, 41</sup> It follows from these examples that if there are sufficiently long growth times in the ultrasonic field the bubbles may interact with one another and combine.

*Repetition rates of USBCs. Time of recompression of bubbles.* The cycling rate at which an USBC may operate under a many-period regime is determined theoretically by the time of establishment and decay of the ultrasonic field in the working volume.<sup>45</sup> In practice, the repetition rate of an USBC, like that of an ordinary bubble chamber, depends on the time of recompression of all the bubbles formed in its working volume. Of decisive importance is the time of recompression of the parasitic-boiling bubbles on the surface of mechanical parts. In the case of USBCs, these bubbles form primarily on the surface of the radiators and on supporting parts due to the release of heat. The recompression time of the bubbles depends on their size and the static excess pressure  $\Delta p_0$  in the liquid. In some experiment the practically achievable repetition rate of the USBC was estimated. In the helium USBC investigated in Ref. 30, the bubble recompression time was determined as follows. The radiators were excited by two ultrasonic pulses (duration 1–1.5 msec) separated by a certain variable time interval  $\Delta t$ . At the end of each pulse, the working volume was photographed. The recompression time was determined from the disappearance of the bubbles on each successive photograph after the fore-



going excitation by the ultrasound. The experiments showed that at  $T_0 = 3.23^\circ\text{K}$  ( $p_0 \approx 0.33$  atm),  $\Delta p_0 \approx 0.13$  atm, and  $\Delta t = 25$  msec the recompression was complete. This shows a chamber can be cycled under these conditions at  $\sim 40$  Hz. At  $T_0 = 3.26^\circ\text{K}$  ( $p_0 \approx 0.35$  atm),  $\Delta p_0 \approx 0.2$  atm, complete recompression was observed at  $\Delta t = 10$  msec, which corresponds to cycling the chamber at  $\sim 100$  Hz.

For the hydrogen USBC used in Refs. 39 and 45 it was noted that at  $T_0 = 25^\circ\text{K}$ , ( $p_0 = 3.2$  atm),  $\Delta p_0 = 0.6$  atm, and  $p_m > 2.8$  atm the bubbles disappeared in a time that did not exceed 15 msec, which indicates a possibility of cycling at 50–100 Hz.

The time for which an USBC can operate at such repetition rates depends on the stability of its temperature regime, which is determined by the heat dissipation in the radiators. As was shown by the experiment<sup>30</sup> made in a helium USBC at repetition frequency 50 Hz and  $\Delta p_0 \approx 0.12$  atm, boiling was not observed on the surface of the radiators during a period of 10 min, i.e., during 30 000 ultrasound pulses. More serious complications may arise in a liquid hydrogen USBC, in which stronger ultrasonic fields are required.

### 3. THEORETICAL INVESTIGATIONS OF THE DYNAMICS OF VAPOR BUBBLES IN AN ULTRASONIC FIELD

#### System of equations describing the pulsations of vapor bubbles in an ultrasonic field

The dynamics of vapor bubbles in an USBC is essentially connected with processes of heat and mass exchange on their surface under the influence of the ultrasonic field. The system of equations that describes the change in time of the radius of a vapor bubble in a liquid under static tension was first formulated in Ref. 46 under various restrictions and simplifications. Subsequently,<sup>47–50</sup> this system was taken as a basis and used to describe the dynamics of vapor bubbles in a liquid subjected to an ultrasonic field. Workers from the Joint Institute for Nuclear Research and the Acoustics Institute<sup>48–50</sup> considered theoretically the nonstationary growth of pulsating vapor bubbles from microscopic size to a visible size. They were studying here a new physical phenomenon of rectified heat transfer due to the growth of vapor bubbles in an ultrasonic field of finite amplitudes.

We give there the most complete system of equations, which includes the equations of the dynamics of the liquid and the vapor, and also the equations of mass and heat transfer. If the liquid is assumed incompressible, the dynamical equations of the liquid reduce to

$$\dot{U}R + 2UR - U^2/2 + [p_\infty(t) - p_R + 2\sigma(1 - \rho'/\rho)^{-1}/R]/\rho = 0; \quad (7)$$

$$u(r, t) = UR^2/r^2; \quad r \geq R, \quad (8)$$

where  $R$ , the radius of the bubble, is a function of the time  $t$ ;  $p_\infty(t)$  is the pressure in the liquid determined by the static pressure  $p_0$  and the pressure of the ultrasonic field with amplitude  $p_m$  and frequency  $\omega = 2\pi f$ , so that  $p_\infty(t) = p_0 - p_m \sin \omega t$ ;  $p'_R$  is the vapor pressure on the surface of the bubble;  $\sigma$  is the surface tension of the liquid;

$\rho'$  and  $\rho$  are the densities of the vapor and the liquid. (Throughout, the primes mean that the corresponding parameters refer to the vapor.) Phase transitions on the surface of the bubble result in a difference between the velocity  $\dot{R}$  of the surface and the velocity of the small particles of the liquid  $U$  and the vapor  $U'$  on this surface, so that the flux of evaporating or condensing matter on the surface is

$$j = (d\mathcal{M}'/dt)/\{4\pi R^2\} = \rho(\dot{R} - U) = \rho'(\dot{R} - U'), \quad (9)$$

where  $\mathcal{M}'$  is the mass of the vapor in the bubble. The vapor pressure  $p'_R$  is determined by the temperature  $T_R$  of the liquid on the boundary of the bubble. If it is assumed that the phase transitions are in equilibrium, then it is easy to find a connection between  $p'_R$  and  $T'_R$ :

$$p'_R = p_\sigma(T_R), \quad (10)$$

and this can be expressed analytically in the form of the Clausius-Clapeyron equation or obtained experimentally. (The index  $\sigma$  indicates that the corresponding function is taken at phase equilibrium of the liquid and vapor.)

To determine the temperature in the liquid and on the boundary of the bubble, it is necessary to solve the heat conduction equation

$$\partial T/\partial t + (u \nabla) T = \nabla(\kappa \nabla T)/\rho c_p, \quad r \geq R, \quad (11)$$

where  $c_p$  is the specific heat of the liquid;  $\kappa$  is the coefficient of thermal conductivity of the liquid; and  $u$  is the velocity of the liquid at the point  $r$ .

Within the bubble, the following equations hold for the vapor when allowance is made for its compressibility:

$$\partial u'/\partial t + (u' \nabla) u' = -\nabla p'/\rho', \quad r < R; \quad (12)$$

$$\partial \rho'/\partial t + (u' \nabla) \rho' u' = 0, \quad r < R; \quad (13)$$

$$\partial s'/\partial t + (u' \nabla) s' = \nabla(\kappa' \nabla T')/\rho' T', \quad r < R; \quad (14)$$

where  $s'$  is the specific entropy of the vapor. The boundary conditions for Eqs. (10) and (13) can be specified in the form  $T_R = R(R, t) = T'(R, t)$ ,  $T(\infty, t) = T_0$ . In addition, it is necessary to give the energy balance equation for the evaporation and condensation on the moving boundary of the bubble:

$$jL = \kappa(\nabla T)_R - \kappa'(\nabla T')_R - \frac{T_R}{R^2} \frac{d}{dt} \left( R^2 \frac{d\sigma}{dT} \right). \quad (15)$$

Writing down the equation of state of the vapor in the bubble,

$$p' = p'(\rho', T'), \quad (16)$$

we close the system of equations (7)–(16).

This system of equations can be simplified by ignoring the inhomogeneity of the temperature within the bubble, which is justified at bubble radii  $R$  much less than the length of the thermal diffusion layer in the vapor, which is  $(2D'/\omega)^{1/2}$ , where  $D'$  is the coefficient of thermal diffusivity of the vapor. For bubbles in liquid hydrogen at  $T_0 = 27^\circ\text{K}$  and frequencies of the ultrasonic field around 40 kHz, this condition is satisfied at radii  $R < 10^{-4}$  cm, i.e., during the initial stage of growth of the cavitation nuclei. At the same time, the condition of

homobaricity within the bubble is satisfied. Then there is no need to solve the problem for  $r < R$ , i.e., Eqs. (12)–(14) can be removed from the system (7)–(16), and Eq. (15) transformed to

$$jL = \kappa (\nabla T)_R - \frac{c'_g \mathcal{H}'}{4\pi R^2} \frac{dT_R}{dt} - \frac{T_R}{R^2} \frac{d}{dt} \left( R^2 \frac{d\sigma}{dT} \right), \quad (17)$$

where  $c'_g$  is the specific heat of the vapor along the phase equilibrium curve;  $\mathcal{H}' = (4/3)\pi R^3 \rho'$ .

Thus, the simplified system of equations that characterizes the dynamics of a thermally uniform vapor bubble includes Eqs. (7)–(11), (16), and (17). This system was first investigated in connection with problems of ultrasonic bubble chambers in Refs. 48–50, and then later in Refs. 51–60. It should be said that even with this simplification of the system of equations it is extremely difficult to obtain an analytic solution of it, and the system must be solved either numerically or approximately. The more general system of equations (7)–(16) was formulated and investigated in Refs. 61 and 62.

#### Analytic solutions. Growth of bubbles due to rectified heat transfer in the ultrasonic field

Analytic solutions of the complete system of equations (7)–(16) can be obtained approximately in the framework of perturbation theory. Suppose that the pressure in the liquid at infinity and on the surface of the bubble varies with the time as

$$p_\infty(t) = p_0 + p_m \exp(i\omega t). \quad (18)$$

We then seek a solution for the bubble radius in the form of a sum of slowly varying and rapidly varying function of the time<sup>61, 62</sup>:

$$R(t) = \overline{R(t)} + R_m(t) \exp(i\omega t) \quad (19)$$

under the condition that  $|R_m| < \overline{R}$ , where  $\overline{R(t)}$  is the value of the radius averaged over a period of the field;  $R_m(t)$  is the amplitude of the pulsations of the radius with the frequency  $\omega$  of the ultrasonic field. We also assume that the mass of the vapor in the bubble is  $\mathcal{H}'(t)$ , its density  $\rho'(r, t)$ , and temperature  $T(r, t)$ , and that the other time-dependent parameters can be expressed in a form analogous to (19), i.e.,

$$\mathcal{H}'(t) = \overline{\mathcal{H}'(t)} + \mathcal{H}'_m(t) \exp(i\omega t); \quad (20)$$

$$\rho'(r, t) = \overline{\rho'(r, t)} + \rho'_m(r, t) \exp(i\omega t); \quad (21)$$

$$T(r, t) = \overline{T(r, t)} + T_m(r, t) \exp(i\omega t). \quad (22)$$

In the linear approximation, one can find the following expressions for  $R_m$  and  $T_m$ :

$$R_m = -p_m K \overline{R} / 3Q; \quad (23)$$

$$T_m = (p_m / Q) (dT/dP)_\sigma, \quad (24)$$

where  $Q$  is a factor that takes into account the resonance characteristics of the bubble and  $K$  is its compressibility. Thus, the amplitude  $R_m$  of the bubble pulsations depends linearly on the mean radius  $\overline{R}$ , the pressure amplitude  $p_m$  of the ultrasonic field, and the bubble compressibility  $K$ , but it is inversely proportional to the factor  $Q$ . The

temperature  $T_m$  also depends linearly on  $p_m$  and is inversely proportional to  $Q$ .

The expression for  $K$  in most general form is

$$K = \frac{1}{R} \left( \frac{dT}{dP} \right)_\sigma \left\{ -\frac{3c'_p}{\omega^2 \alpha' T} \left( 1 + i \frac{D'}{\omega} w_1^2 + i \frac{\omega \alpha' T D'}{L} \right) \times \left( \frac{1}{2} + C \right) \frac{1}{R} f(w_1 \overline{R}) - \frac{3c'_p}{\omega^2 \alpha' T} \left( 1 + i \frac{D'}{\omega} w_2^2 + i \frac{\omega \alpha' T D'}{L} \right) \left( \frac{1}{2} - C \right) \frac{1}{R} f(w_2 \overline{R}) + \frac{3}{2} \frac{\rho c_p}{\rho' L} \left( \frac{2D}{\omega} \right)^{1/2} \left[ 1 - i - i \frac{(2D/\omega)^{1/2}}{R} \right] \right\}, \quad (25)$$

where  $w_1$  and  $w_2$  are related to the length of the temperature wave [which is of order  $(2D'/\omega)^{1/2}$ ] and the acoustic wavelength  $\lambda_v$  in the vapor by

$$w_1 \approx \frac{1+i}{\sqrt{2D'/\omega}} \left[ 1 + i\pi(\gamma-1) \frac{2D'/\omega}{\lambda_v^2} \right], \quad w_2 \approx i2\pi/\lambda_v; \quad (26)$$

$c'_p$  is the specific heat of the vapor;  $\alpha'$  is the coefficient of thermal expansion of the vapor; and  $D$  is the coefficient of thermal conduction of the liquid. The function

$$f(w \overline{R}) = w \overline{R} \coth(w \overline{R}) - 1, \quad (27)$$

and the constant  $C$  can be expressed in the form  $C \approx (c'_g/c'_p - 1/2)$  under the condition  $(2D'/\omega)^{1/2} < \lambda_v$ , which is usually satisfied at frequencies  $f \ll 10^{12}$  Hz.

The factor  $Q$  can be expressed in the form<sup>55</sup>

$$Q = 1 - (\rho \omega^2 \overline{R}^2 + 2\sigma/\overline{R}) (K/3). \quad (28)$$

The function  $Q$  is complex. At a definite frequency  $\omega = \omega_0$  of the acoustic field,  $|Q|$  is minimal, and in this case  $\omega_0$  determines the frequency of resonance pulsations of the vapor bubble. The frequency of the resonance pulsations of the bubble radius in the general case may differ from the characteristic frequency, and it is determined by the condition of maximum of the ratio  $|R_m|/\overline{R}$ . Therefore, in accordance with (23), the resonance frequency  $\omega_0$  is determined in general form by the expression

$$\frac{d}{d\omega} (|K/Q|)_{\omega=\omega_0} = 0. \quad (29)$$

Usually, the frequency  $\omega_c$  of characteristic pulsations is very close to the resonance frequency  $\omega_0$ . In the case when  $\text{Re}K$  depends weakly on  $\omega$ , the resonance frequency of the vapor bubble is equal to the characteristic frequency, and it can be determined from the condition  $\text{Re}Q \approx 0$ . For the resonance frequency, one can then obtain the expression<sup>54, 55</sup>

$$\omega_0^2 = (3/\text{Re}K - 2\sigma/\overline{R})/\rho \overline{R}^2. \quad (30)$$

The dependences of the resonance frequencies on the radii of vapor bubbles in liquid hydrogen and liquid helium are given in Fig. 21.

It should be pointed out that at frequencies  $\omega$  of the ultrasonic field appreciably lower than the resonance frequency  $\omega_0$  the value of  $Q$  tends to unity,  $Q \rightarrow 1$ . In this case, the theoretical treatment of the dynamics of the vapor bubbles simplifies. In the experiments of Refs. 34, 35, and 39, bubbles with sizes less than and



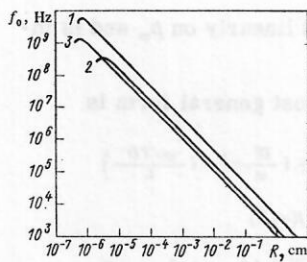


FIG. 21. Radial dependence of the resonance frequency of vapor bubbles for different liquids (Refs. 54 and 63). 1) Liquid hydrogen at 27 °K; 2) at 20.3 °K; 3) liquid helium at 4.2 °K.

greater than the resonance size were observed. In Ref. 35, in which liquid hydrogen was excited by an ultrasonic field with frequency  $\sim 40$  kHz, the bubbles grew to a size of order  $10^{-2}$  cm, i.e., they did not reach the resonance value, which is approximately equal to  $10^{-1}$  cm at that frequency. In other experiments,<sup>34,39</sup> the frequency of the ultrasonic field was  $\sim 300$  kHz and exceeded the resonance frequencies of the observed bubbles. Note that in such a case the absorption of ultrasound in the liquid can increase considerably, and there may also be a stronger interaction between individual bubbles, resulting in their combining.

To determine the mean radius  $\bar{R}(t)$  of the growing bubble, it is necessary to solve the nonstationary problem of the dynamics of the bubble in the ultrasonic field. In the quadratic approximation in the framework of perturbation theory, the solution for the rate of change of the mean radius in time is<sup>60-62</sup>

$$\begin{aligned} \frac{d\bar{R}}{dt} = \frac{\kappa}{\rho' L \bar{R}} \left\{ -\frac{P_m^2}{4|Q|^2} \left( \frac{d^2 T}{dp^2} \right)_\sigma - \frac{|T_m|^2}{4\kappa} \left( \frac{d\kappa}{dT} \right)_\sigma - \right. \\ \left. - 2 \operatorname{Re} \left[ \frac{T_m R_m^*}{\bar{R}} (1 - 3F_5) \right] + \omega \frac{\operatorname{Im}(\phi_m' T_m^*)}{8\pi\kappa\bar{R}} \right. \\ \left. \times \left[ -c'_0 + \left( \frac{dL}{dT} \right)_\sigma \right] + \frac{\omega c_p}{8\pi\kappa\bar{R}} \operatorname{Im}[\phi_m' T_m^* (1 - F_5)] \right. \\ \left. - \frac{P_m^2}{|Q|^2} \frac{\rho\omega^2}{36} \bar{R}^2 |K|^2 \left( \frac{dT}{dp} \right)_\sigma - \left( \Delta p_0 + \frac{2\sigma}{\bar{R}} \right) \left( \frac{dT}{dp} \right)_\sigma \right\}, \quad (31) \end{aligned}$$

where  $\Delta p_0$  is the static excess pressure of the liquid defined by  $\Delta p_0 = p_0 - p_\sigma(T_0)$ ;  $F_3$  and  $F_5$  are the functions given by

$$F_n = F_n(y) = \int_0^\infty \frac{\exp[-(1+i)zy]}{(1+z)^n} dz; \quad y = \frac{\bar{R}}{\sqrt{2D/\omega}}. \quad (32)$$

If the expression in the curly brackets in (31) is greater than zero, then the mean radius  $\bar{R}(t)$  increases in time because of nonlinear mechanisms in the ultrasonic field which give rise to a new phenomenon in pulsations of vapor bubbles.<sup>48-63</sup> This phenomenon, which has become known as *rectified heat transfer*,<sup>62,66</sup> characterizes the growth of the vapor bubble due to the time-averaged flow of heat into it from the liquid. It has a certain analogy with the phenomenon of rectified gas diffusion responsible for the growth of gas bubbles in water under the influence of an ultrasonic field.<sup>64,65</sup>

Let us consider the physical mechanisms that govern the growth of vapor bubbles in an ultrasonic field due to rectified heat transfer. We note first of all that if the conditions of phase equilibrium are satisfied on the bubble surface, the temperature varies in accordance with (22) and (24) corresponding to the change in the pressure

(18). When a bubble expands in an ultrasonic field, the temperature on its surface satisfies  $T_1 < T_0$ , and when it contracts,  $T_2 > T_0$ . The differences  $T_0 - T_1$  and  $T_0 - T_2$  determine the temperature gradients on the bubble surface. The heat flux into and out of the bubble is related to the magnitude and direction of these gradients and also the surface area of the bubble.

The first term in the curly brackets in (31) governs the growth of the vapor bubble due to the nonlinearity of the phase equilibrium curve, since  $(d^2 T/dp^2)_\sigma < 0$ . Physically, this has the consequence that during the expansion phase of the bubble, when the heat flux is from the liquid, the temperature gradient is in absolute magnitude greater than during the compression phase, when the heat flux is into the liquid. Because of this, over the period of the ultrasonic field there is a net average flux of heat from the liquid to the bubble, and this leads to the evaporation of liquid on the surface and an increase in the mean radius  $\bar{R}(t)$  of the bubble. The second term takes into account the dependence of  $\kappa$  on  $T$ , though its influence on the bubble growth is insignificant. The third term determines the growth of the bubble caused by the difference between the heat fluxes through its surface during the expansion and contraction phases due to the fact that during the expansion phase the surface of the bubble is on the average greater than during the contraction phase. This mechanism is analogous to the one observed for gas bubbles in an ultrasonic field growing as a result of the phenomenon of rectified gas diffusion.<sup>64,65</sup> The following terms also characterize growth of the vapor bubble. The mechanism of this growth is due to the release, on the average, of heat in the vapor bubble as a result of the work done on it by the ultrasonic field. The mechanisms described by the last two terms in the curly brackets of (31) hinder this growth of the vapor bubble. The penultimate term takes into account the influence of the inertial terms of the equation of motion and determines the dynamic pressure excess of the liquid hindering the bubble growth in the ultrasonic field. This is important at high pulsation velocities of a vapor bubble, which occur, for example, when the bubbles have sizes near the resonance value. The last term takes into account the static excess pressure of the bubble ( $\Delta p_0 + 2\sigma/\bar{R}$ ), which is the main hindrance to its growth. It is easy to see that this term does not depend on the pressure amplitude  $p_m$  of the ultrasonic field. Therefore, with increasing amplitude  $p_m$  one can always reach a regime in which the growth mechanisms predominate over the mechanisms of collapse due to the static overpressure effects on the bubble.

Equation (31) in the case of a small static excess pressure can be simplified and its solution represented in the form of multiple relations. For small vapor bubbles, when the first three terms in the curly brackets of (31) are important, one can write the time dependence of the bubble radius in the form

$$\bar{R}(t) \sim A_1 t^{1/2}, \quad (33)$$

where  $A_1$  is a constant. For liquid hydrogen, Eq. (33) holds when  $\bar{R} < 7 \cdot 10^{-4}$  cm. For large bubbles the re-

maining terms are important, and then

$$\bar{R}(t) \sim A_2 t, \quad (34)$$

where  $A_2$  is a constant. The constants  $A_1$  and  $A_2$  are related to the amplitude and frequency of the ultrasonic field and also to the thermodynamic parameters of the liquid. They can be expressed in the form  $A_1 = C_1 p_m$ ,  $A_2 = C_2 \sqrt{\omega} p_m^2$ , where in the case of liquid hydrogen at  $T_0 = 27^\circ \text{K}$  the two constants have the value  $C_1 \approx 0.3 \cdot 10^{-7} \text{ cm}^3 \cdot \text{dyn}^{-1} \cdot \text{sec}^{-1/2}$  and  $C_2 \approx 0.7 \cdot 10^{-15} \text{ cm}^5 \cdot \text{dyn}^{-2} \cdot \text{sec}^{-1}$  (Ref. 61).

At bubble radii  $\bar{R}$  exceeding the resonance values,  $R_m$ ,  $T_m$ , and  $\omega'_m$  are decreased by the increase in the factor  $Q$ , and therefore, above a certain size of the bubbles, the effects of rectified heat transfer are reduced compared with the effects due to the overpressure, and the bubbles cease to grow further, having reached a certain asymptotic radius  $\bar{R}$ .

### Numerical solutions. Dependence of bubble dynamics on the parameters of the liquid and the ultrasonic field

An analytic and a numerical solution characterizing the growth of a bubble in liquid hydrogen are given in Fig. 22. This shows the dependences of the relative radii  $R/R_0$  on the number of periods  $\omega t/2\pi$  of the ultrasonic field, where  $R_0$  is the initial radius of the bubble. The analytic solution was constructed in accordance with (23) and (31), and the numerical solution found on a computer for the original system of equations (13)–(22). It can be seen from these results that in the numerical solutions there are, besides the pulsation component with the frequency of the ultrasonic field, pulsation components with a higher frequency close to the resonance frequency for a bubble of the given radius.

During the growth of a bubble, the resonance frequency decreases and may approach the frequency  $\omega$  of the ultrasonic field. At the same time, the amplitude of the pulsations increases considerably and the bubble ceases to grow. All this is well illustrated in Fig. 23, which shows numerical solutions of the system of equations (13)–(17), (23), and (24) for a vapor bubble in an

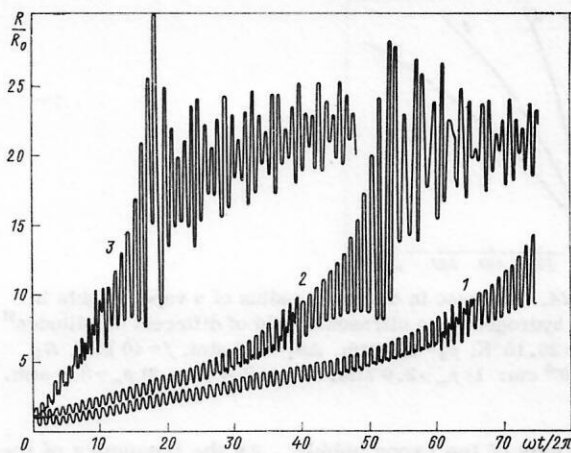


FIG. 23. Pulsations of vapor bubble in liquid nitrogen in an ultrasonic field of different amplitudes at frequency 50 kHz (Ref. 62) at  $T_0 = 77.35^\circ \text{K}$ ,  $p_0 = 1.2 \text{ atm}$ ,  $\Delta p_0 = 0.2 \text{ atm}$ ,  $R_0 = 5 \cdot 10^{-4} \text{ cm}$ : 1)  $p_m = 0.35 \text{ atm}$ , 2)  $p_m = 0.4 \text{ atm}$ , 3)  $p_m = 0.5 \text{ atm}$ .

ultrasonic field of different amplitudes for the case of liquid nitrogen.<sup>59</sup> At a frequency 50 kHz of the ultrasonic field in liquid nitrogen, the resonance radius of a vapor bubble is  $\sim 10^{-2} \text{ cm}$ , and for initial radius  $R_0 = 5 \cdot 10^{-4} \text{ cm}$  this corresponds to  $R/R_0 = 20$ . Figure 23 shows clearly that when the resonance radius is reached the growth of the vapor bubble in the ultrasonic field stops.

With increasing pressure amplitude  $p_m$  of the ultrasonic field, the rate of growth of the mean radius increases, which corresponds to the analytic solutions given above. Numerical solutions characterizing the increase with time of the mean radius  $\bar{R}(t)$  of the vapor bubble in liquid hydrogen under the influence of an ultrasonic field of frequency 40 kHz (Ref. 51) are given in Fig. 24, from which it can be seen that with increasing pressure amplitude of the ultrasonic field the rate of growth  $d\bar{R}/dt$  of the mean bubble radius increases.

Numerical solutions obtained at a given frequency of the ultrasonic field can be generalized to the case of other frequencies by using the self-similarity of the solutions,<sup>56</sup> since the function

$$F(\omega t/2\pi) = f\bar{R}^2(\omega t/2\pi) \quad (35)$$

has a universal form that does not depend on the frequency  $f$  in a certain range of the argument  $\omega t/2\pi$ , which determines the number of periods of the ultrasonic field. Numerical solutions for a vapor bubble in liquid hydrogen for the same thermodynamic parameters, the same pressure amplitude  $p_m = 2.0 \text{ atm}$  of the ultrasonic field, but different frequencies  $f$  are shown in Fig. 25. It can be seen that if the solutions are represented in the form of the functions (35), the initial growth sections coincide right up to hundreds of periods of the ultrasonic field at different frequencies from 10 to 400 kHz. A deviation, which may be characterized by the extent to which the self-similarity of the functions (35) is violated, begins because of the influence of the inertial terms of the equation of motion, which is manifested in the excitation of characteristic (resonance)

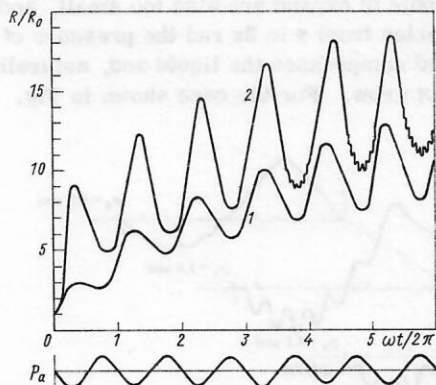


FIG. 22. Comparison of analytic and numerical solutions for pulsations of a bubble in liquid hydrogen in an ultrasonic field with frequency 50 kHz (Ref. 62) at  $T_0 = 27^\circ \text{K}$ ,  $p_0 = 5.0 \text{ atm}$ ,  $\Delta p_0 \approx 0.2 \text{ atm}$ ,  $R_0 = 5 \cdot 10^{-5} \text{ cm}$ ,  $p_m = 3.0 \text{ atm}$ . 1) Analytic solution; 2) numerical solution.



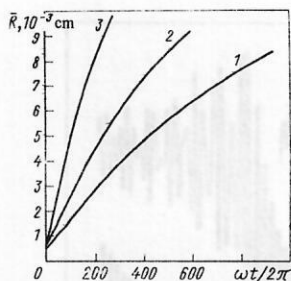


FIG. 24. Increase in the mean radius of a vapor bubble in liquid hydrogen in an ultrasonic field of different amplitudes<sup>51</sup> at  $T_0 = 26.15^\circ\text{K}$ ,  $p_0 = 4.6$  atm,  $\Delta p_0 = 0.5$  atm,  $f = 40$  kHz,  $R_0 = 5 \cdot 10^{-4}$  cm: 1)  $p_m = 2.0$  atm; 2)  $p_m = 2.4$  atm; 3)  $p_m = 3.0$  atm.

pulsations of the vapor bubble. As the frequency of the ultrasonic field is raised, the corresponding resonance radii of the bubbles decrease, and so do the limiting radii to which the vapor bubbles can grow as a result of rectified heat transfer. In this connection, it is of interest to examine the numerical solutions given in Figs. 26 and 27 (Ref. 63). It follows from them that the characteristic pulsations of bubbles of the same radius ( $8 \cdot 10^{-3}$  cm) increase with increasing pressure amplitude of the ultrasonic field and decreasing static pressure excess. It follows from this that the increase in the static excess pressure  $\Delta p_0$  of the liquid and decrease in the amplitude  $p_m$  may increase the asymptotic radius reached by a vapor bubble in the ultrasonic field. At the same time, of course, there will be a decrease in the rate of increase  $dR/dt$  of the mean radius of the vapor bubble, and this must be taken into account when one is selecting regimes of operation of ultrasonic bubble chambers.

As was noted above, a vapor bubble grows in the ultrasonic field because of the rectified heat transfer, which is characterized by the time-averaged flux of heat from the liquid to the bubble and determined by the temperature gradient on its surface. The temperature distributions in the liquid around a bubble at different times  $t_n$  separated by equal intervals equal to  $1/10$  of the period of the ultrasonic field, so that the complete set of distributions characterizes the change in the temperature during one period of the ultrasonic field, are given in Fig. 28 (Ref. 63). In the top left of this figure, we show the corresponding change in the radius of the bubble during this period. This case is characterized by strongly developed characteristic pulsations of the vapor bubble, which in order of magnitude approach the values of the forced pulsations. As can be seen from Fig. 28,

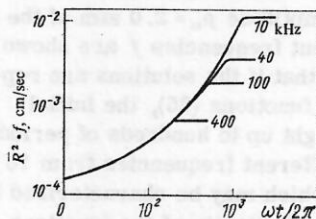


FIG. 25. Growth of vapor bubbles in liquid hydrogen at different frequencies of the ultrasonic field<sup>56</sup> at  $T_0 = 26.15^\circ\text{K}$ ,  $p_0 = 4.6$  atm,  $\Delta p_0 = 0.5$  atm, and  $p_m = 2.0$  atm.

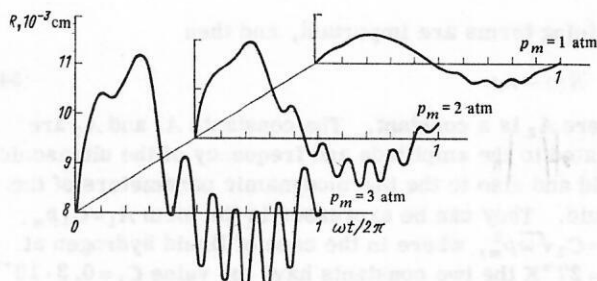


FIG. 26. Pulsations of a vapor bubble in liquid hydrogen at different amplitudes of an ultrasonic field with frequency 40 kHz (Ref. 63) at  $T_0 = 26.15^\circ\text{K}$ ,  $p_0 = 4.6$  atm,  $\Delta p_0 = 0.5$  atm.

the characteristic pulsations of the bubble also begin to be manifested in the distribution of the temperature near the bubble. At certain instants of time, the temperature gradients may be completely determined by the characteristic pulsations of the bubble when the heat flux on its surface changes.

The initial temperature distribution shown in Fig. 28 corresponds to a bubble heated by  $0.5^\circ\text{K}$  relative to the liquid, which was dictated by the choice of the initial temperature condition on its surface, this leading to stable numerical solutions. The stability of the numerical solutions also depends on the initial conditions relating to the phase of the ultrasonic field. The numerical solutions found above were obtained when the pressure of the ultrasonic field has the form

$$p_a = -p_m \sin \omega t. \quad (36)$$

If this pressure is given with a different initial phase  $\varphi$ ,

$$p_a = -p_m \sin(\omega t + \varphi), \quad (37)$$

the solutions are structurally unstable in certain regions of variation of  $\varphi$ . Different numerical solutions for a vapor bubble in liquid hydrogen subjected to an ultrasonic field with different initial phases are shown in Fig. 29 (Ref. 67). The bubble does not grow if the initial phase  $\varphi$  lies in the range from 0 to 0.8, since it is dissolved faster than the pressure decrease in the ultrasonic field can become effective. As the phase is varied from 2 to  $\pi$  rad, the pressure reductions in the liquid needed for the bubble to expand are also too small, and when the phase varies from  $\pi$  to  $2\pi$  rad the pressure of the ultrasonic field compresses the liquid and, naturally, the bubble does not grow. For the case shown in Fig.

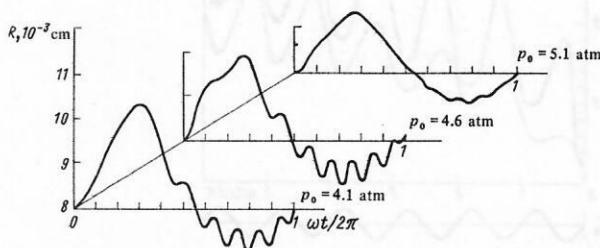


FIG. 27. Pulsations of a vapor bubble in liquid hydrogen in an ultrasonic field with frequency 40 kHz at different static excess pressures (Ref. 63) at  $T_0 = 26.15^\circ\text{K}$ ,  $p_0 = 4.1$  atm,  $p_m = 2.0$  atm.

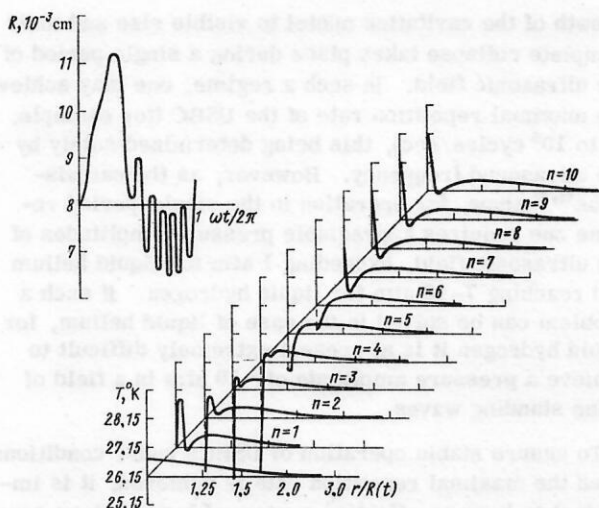


FIG. 28. Temperature distribution in liquid hydrogen near a pulsating bubble at different instants of time during one period of the ultrasonic field (Ref. 63) at  $T_0 = 26.15^\circ\text{K}$ ,  $p_0 = 4.6$  atm,  $\Delta p_0 = 0.5$  atm,  $f = 40$  kHz,  $p_m = 3.0$  atm,  $R_0 = 8 \cdot 10^{-3}$  cm.

29, the bubble grows if the initial phase of the ultrasonic field lies in the interval from 0.8 to 1.8 rad. Naturally, with increasing pressure amplitude of the ultrasonic field, this interval expands, but in the limit it cannot be greater than  $\pi$ .

#### Comparison of theoretical and experimental results. Further investigations of the dynamics of bubbles in USBCs

The available experimental data on the behavior of bubbles in USBCs are as yet insufficient for a detailed comparison with the theoretical ideas so far developed, though it is of interest to make what comparisons we can. The results of calculation of the growth of the bubble radius in a liquid hydrogen USBC with working parameters corresponding to the conditions when tracks of ionizing particles were observed are given in Fig. 30 (Ref. 35). The calculations were made in accordance with Eq. (31). They are shown in the form of the dependence of the mean radius normalized to the length  $(2D/\omega)^{1/2}$  of the thermal diffusion layer in hydrogen on the number of periods of the ultrasonic field. Note that for hydrogen at  $T_0 = 27^\circ\text{K}$  the value of  $(2D/\omega)^{1/2}$  at frequency 38.4 kHz is  $\sim 10^{-4}$  cm. In the experiments, tracks of ionizing particles were observed after two

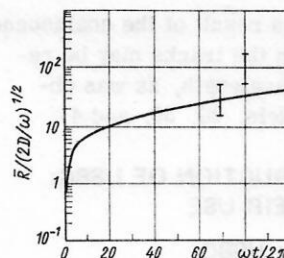


FIG. 30. Comparison of calculations with experimental results for liquid hydrogen USBC at  $T_0 = 27^\circ\text{K}$ ,  $p_0 \approx 5.2$  atm,  $\Delta p_0 = 0.35$  atm,  $f = 38.4$  kHz,  $p_m = 3.0$  atm,  $(2d/\omega)^{1/2} \approx 10^{-4}$  cm.

characteristic time intervals  $\Delta t_2$  (see Fig. 11), which corresponded to 68 and 80 periods of the ultrasonic field. In Table III, we give the radii of the bubbles and also their densities on the tracks corresponding to these growth intervals. It can be seen from this table that with increasing ultrasonic field the bubbles combine, so that during the course of time their density decreases. A similar picture is also observed in ordinary bubble chambers,<sup>68</sup> but in the ultrasonic field the processes of combination take place more strongly since in this case there are several specific mechanisms of combination associated, for example, with Bjerknes, Koenig, and other forces.<sup>27</sup>

Since the theoretical ideas so far developed correspond to pulsations of isolated bubbles in the ultrasonic field and do not take into account their interaction, it would be of interest to study in more detail both experimentally and theoretically the effects of this interaction.

Another problem requiring further investigation in the dynamics of vapor bubbles in an ultrasonic field may be concerned with the fact that, besides radially symmetric pulsations, the bubbles may execute oscillations which cause a loss of their spherical symmetry. Such oscillations may be responsible for the creation near bubbles of microfluxes resulting in intense heat exchange with the liquid. By analogy with the influence of these effects on the growth of gas bubbles in an ultrasonic field,<sup>69</sup> they may have an important influence on the dynamics of the vapor bubbles, increasing the average rate of their growth.

When ultrasonic fields of high frequencies (higher than 200–300 kHz) are used in USBCs, the radii of the optically observable bubbles will correspond to the resonance radii or exceed them. The velocity with which the surface of the bubbles pulsating under these conditions moves may be so large that it will lead to a strong influence of the compressibility and viscosity of the liquid and also to a strong manifestation of the interac-

TABLE III. Sizes and densities of bubbles on tracks of ionizing particles at different intervals of time during the growth in an ultrasonic field.

Interval of time during growth		Radius $\bar{R}$ , $10^{-2}$ cm	Density of bubbles, $\text{cm}^{-1}$
msec	Number of periods of ultrasonic field		
1.77	68	0.2–0.5	30–40
2.08	80	0.5–3.0	7–18

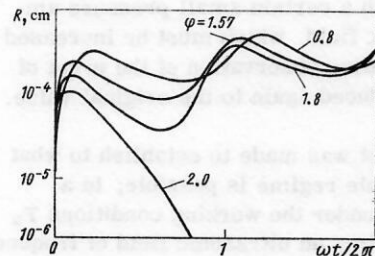


FIG. 29. Variation in time of the radius of a vapor bubble in liquid hydrogen for different initial phases (in radians) of the ultrasonic field<sup>67</sup> at  $T_0 = 24.6^\circ\text{K}$ ,  $p_0 = 3.4$  atm,  $\Delta p_0 = 0.4$  atm,  $f = 300$  kHz,  $p_m = 2.5$  atm,  $R_0 = 2 \cdot 10^{-6}$  cm.



tion of the bubbles. Then, as a result of the coalescence of the bubbles, their density on the tracks may be reduced to a single bubble per wavelength, as was observed in the experiments of Refs. 29, 39, and 41.

#### 4. ASPECTS OF THE CONSTRUCTION OF USBCs AND POSSIBILITIES FOR THEIR USE

##### Formation of ultrasonic fields in USBCs

We have considered above two ways of producing an ultrasonic field in USBCs—by means of a focusing ultrasonic system and by means of planar ultrasonic radiators. As can be seen in Fig. 14, the ultrasonic field produced by a focusing system is characterized by spatial inhomogeneity, which leads to differences in the density of the tracks along their length (see Fig. 15). In some cases, for example, when an USBC is used as a detector-cum-target, such an inhomogeneity is not important. However, for high quality detection of tracks it is clearly better to generate the ultrasonic field by means of planar radiators. Experiments show<sup>35, 45</sup> that even in this case it is difficult to obtain the required uniformity of the ultrasonic field. If the amplitude  $p_m$  of the ultrasonic pressure only slightly exceeds the threshold value  $p_{m,cr}$  (as, for example, in the case of liquid hydrogen), then a large part of the working volume of the USBC is insensitive to ionizing radiation. This was clearly demonstrated by the experiment of Ref. 35, the results of which are presented in Fig. 19. The beam of pions from the accelerator had a cross section with characteristic diameter of about 6 cm before it entered the bubble chamber, but in the ultrasonic field the region sensitive to the particle beam measured only about 2–3 cm. Only some of the particles, those moving near the axial line of the radiating system where the pressure amplitude of the ultrasonic field was maximal, were detected. In this connection, it is evidently expedient to generate plane standing waves in the USBC by means of antenna systems composed of many individual radiators on whose surface one can adjust the pressure amplitude by applying different voltages.

A field of plane standing waves has a shortcoming due to the fact that in the transverse direction, along the planes of the nodes of the standing waves, there are regions which are insensitive to the ionizing radiation. If the ultrasonic wavelength is of the order of several centimeters, this region is fairly large, and particles moving through it will not be detected in the chamber. In this case, one can use combined ultrasonic antenna systems that produce fields of standing waves in mutually perpendicular directions. It is helpful to use them in large USBCs, in which one would not want to use very high frequencies in order to avoid appreciable absorption of the ultrasound during its propagation.

##### Repetition rate of USBCs. Temperature control

As we have noted above, for an USBC operating under a many-period pulse regime, a repetition rate of about 50–100 cycle/sec was in practice achieved for a time of ~10 min. At present, no experimental data are available on operation in a single-period regime when the

growth of the cavitation nuclei to visible size and their complete collapse takes place during a single period of the ultrasonic field. In such a regime, one may achieve the maximal repetition rate of the USBC (for example, up to  $10^6$  cycles/sec), this being determined solely by the ultrasound frequency. However, as the calculations<sup>45, 63</sup> show, for operation in the single-period regime one requires appreciable pressure amplitudes of the ultrasonic field, exceeding 1 atm for liquid helium and reaching 7–10 atm for liquid hydrogen. If such a problem can be solved in the case of liquid helium, for liquid hydrogen it is at present extremely difficult to achieve a pressure amplitude of ~10 atm in a field of plane standing waves.

To ensure stable operation of USBCs under conditions when the maximal repetition rate is achieved, it is important to have an effective system of temperature control. Since the principal dissipation of heat takes place within the ultrasonic radiators, its removal is an important problem. In this connection, the USBC construction proposed in Ref. 71 warrants attention; in it, it is proposed that the ultrasonic radiator be placed in a thermostatically controlled box that is separated from the working volume and filled with a medium having a high cavitation threshold.

Obviously, it is hardest to remove the heat in large USBCs (larger than 1 m), in which it is necessary to use ultrasonic generators of high power to excite the ultrasonic systems. In this case, the only way to operate the USBC is clearly in a pulsed regime.

##### USBCs with memory. On the possibility of realizing a "controllable" regime

As theoretical investigations show (see, for example, Fig. 24), the rate of growth of the bubbles due to rectified heat transfer in the ultrasonic field is slower, the smaller is the pressure amplitude  $p_m$ . It is a reasonable conjecture that when an ultrasonic field is excited with pressure amplitude  $p_m$  slightly exceeding the threshold value  $p_{m,cr}$ , the cavitation nuclei will grow at a very slow rate. At a certain amplitude  $p_m \approx p_{m,cr}$  the bubbles may pulsate in the ultrasonic field for a considerable time without reaching visible size,<sup>50, 51</sup> i.e., at this amplitude the USBC may "remember" the tracks of the ionizing particles. Such a regime is of interest from the point of view of selecting useful events. To a certain extent, it is analogous to a controllable regime with the only difference that in this case the chamber operates in a waiting regime with a certain small pressure amplitude of the ultrasonic field, which must be increased at the right time, and after observation of the event of interest the field is reduced again to the original value.

In Ref. 22, an attempt was made to establish to what extent such a controllable regime is possible; in a Freon bubble chamber under the working conditions  $T_0 = 26^\circ\text{C}$  and  $p'_0 \approx p_g = 23$  atm, an ultrasonic field of frequency 25 kHz and amplitude  $p_m \approx 5$  atm was generated. Under these conditions, and under the influence of the ultrasound and  $\gamma$  rays from a  $^{60}\text{Co}$  source, the liquid was mechanically stressed in the chamber and the working

volume photographed and then the procedure was repeated without ultrasound. If the ultrasonic field can increase the time of existence of the cavitation nuclei, then in the first regime one should observe more bubbles than in the second. However, in the experiment this was not observed, which could be explained by the fact that pressure amplitude  $p_m$  was almost two times smaller than the threshold value  $p_m$  for Freon under these conditions.

### On the possibility of using USBCs in "hybrid" installations

As we said above, there has recently been considerable development in high energy physics of hybrid installations that combine the advantages of bubble chambers and electronic methods of detection with fast response.

In a hybrid system the bubble chamber is used as a sensitive target, which permits one to determine with high accuracy the coordinates of the interaction vertex and also the angles of emission and the momenta of secondary particles with short ranges. The remainder of the system consists of spark, wire, and drift chambers, Čerenkov spectrometers, etc., which must carry out a preliminary analysis and selection of detected events, and then send a command for photographing of the events of interest and measure the energy and kinematic parameters of the secondary high energy particles.

As was pointed out in Ref. 38, bubble chambers in hybrid systems must have a repetition rate not lower than 50 cycle/sec, and the characteristic size of the working volume must be more than 10 cm. In addition, the walls of the chamber in the direction of exit of the secondary particles must be thin. It follows from the results given above that already at the present state of their development USBCs can satisfy the requirements for chambers used in hybrid systems.

### CONCLUSIONS

On the basis of the results of investigations reviewed here, we can say that the construction of ultrasonic bubble chambers is basically possible. If USBCs are to become working instruments, it will be necessary to solve many technical tasks and problems, which, however, are no longer of a fundamental nature at the present time. Their solution largely depends on the development of ultrasonic technology, which we may expect to solve problems such as the development of new high efficiency piezoceramic materials for low temperature liquids, a technology for preparing composite radiators for USBCs, the construction of ultrasonic systems with uniform distribution of the field amplitude over a surface, and so on.

It is a pleasant duty to thank V. G. Grebinnik, A. Yu. Didyk, A. P. Manych, A. F. Pisarev, A. I. Filippov, and V. D. Shestakov at the Joint Institute for Nuclear Research, V. N. Alekseev, V. A. Bulanov, L. P. Gavrilov, A. M. Kopov, V. A. Krasil'nikov, L. M. Lyamshchev, L. O. Makarov, K. A. Naugol'nykh, M. G. Sirotuk, and V. P. Yushin at the Acoustics Institute, G. I.

Selivanov at the Institute of High Energy Physics, Serpukhov, and also V. K. Lyapidevskii at the Moscow Engineering Physics Institute for many discussions of the results presented here and for ideas. We also thank V. P. Dzhelepov and B. M. Pontecorvo for interest in the work.

- <sup>1</sup>G. H. Trilling, in: Proc. Intern. Conf. Bubble Chamber Technology, Argonne Natl. Lab. (1970), p. 1173; C. M. Fisher, in: Intern. Conf. Instrum. for High Energy Physics, Frascati, Italy (1973), p. 21.
- <sup>2</sup>Yu. A. Budagov *et al.*, Nucl. Instrum. Methods **20**, 128 (1963); R. D. Watt, in: Intern. Conf. Instrum. for High Energy Physics, Frascati (1973), p. 44.
- <sup>3</sup>A. Rogers, in: Proc. Intern. Conf. Bubble Chamber Technology, Argonne Natl. Lab. (1970), p. 346; V. A. Bogach, Avt. Svid (Author's Certificate) No. 241551. Byull. Izobretenii, No. 14 (1969).
- <sup>4</sup>F. Seitz, Phys. Fluids **1**, 2 (1958).
- <sup>5</sup>N. A. Roĭ, Akust. Zhurn. **3**, 3 (1957).
- <sup>6</sup>M. G. Sirotuk, Akust. Zhurn. **8**, 255 (1962).
- <sup>7</sup>V. A. Akulichev and M. G. Sirotuk, Tr. Akusticheskogo Instituta **3**, 80 (1967).
- <sup>8</sup>Yu. A. Aleksandrov *et al.*, Puzyr'kovye Kamery (Bubble Chambers, Bloomington (1968)), Gosatomizdat, Moscow (1963).
- <sup>9</sup>A. G. Tenner, Nucl. Instrum. Methods **22**, 1 (1963).
- <sup>10</sup>N. B. Vargaftik, Spravochnik po Teplofizicheskim Svoistvam Gazov i Zhidkosti (Handbook of Thermal and Physical Properties of Gases and Liquids), Nauka, Moscow (1972).
- <sup>11</sup>V. A. Akulichev and V. A. Bulanov, Zh. Eksp. Teor. Fiz. **65**, 668 (1973) [Sov. Phys. JETP **38**, 329 (1974)].
- <sup>12</sup>V. A. Akulichev and V. A. Bulanov, Akust. Zhurn. **20**, 817 (1974).
- <sup>13</sup>D. V. Lieberman, Phys. Fluids **2**, 466 (1959).
- <sup>14</sup>D. Sette and F. Wanderlingh, **125**, 409 (1962).
- <sup>15</sup>D. Messinò, D. Sette, and F. Wanderlingh, J. Acoust. Soc. Amer. **35**, 1575 (1963).
- <sup>16</sup>D. Messinò, D. Sette, and F. Wanderlingh, J. Acoust. Soc. Amer. **35**, 926 (1963).
- <sup>17</sup>R. D. Finch, J. Acoust. Soc. Amer. **36**, 2287 (1964).
- <sup>18</sup>B. Hahn, Nuovo Cimento **22**, 650 (1961).
- <sup>19</sup>B. Hahn and R. N. Peacock, Nuovo Cimento **28**, 334 (1963).
- <sup>20</sup>M. Bertolotti and D. Sette, Nuovo Cimento **32**, 1182 (1964).
- <sup>21</sup>A. L. Hughes, in: Proc. Intern. Conf. Instrum. for High Energy Physics, Berkeley (1960), p. 99.
- <sup>22</sup>V. K. Lyapidevskii, R. M. Sulyaev, and I. V. Palomkin, Preprint JINR No. 884 [in Russian], Dubna (1962).
- <sup>23</sup>Yu. A. Aleksandrov, G. S. Voronov, and N. B. Delone, Zh. Eksp. Teor. Fiz. **43**, 1552 (1962) [Sov. Phys. JETP **16**, 1095 (1963)].
- <sup>24</sup>C. West, Nucl. Instrum. Methods **33**, 361 (1965).
- <sup>25</sup>M. Bertolotti, D. Sette, and F. Wanderlingh, Nucl. Instrum. Methods **35**, 109 (1965).
- <sup>26</sup>P. De Santis, D. Sette, and F. Wanderlingh, Nucl. Instrum. Methods **55**, 189 (1967).
- <sup>27</sup>L. Bergmann, Ultrasonics and their Scientific and Technical Applications, U. S. Govt. Print. Off., Washington (1951) [Russian translation from German original: Izd-vo Inostr. Lit. (1957)].
- <sup>28</sup>Y. Kikuchi, in: Ultrasonic Transducer Materials (ed. R. Belincourt), New York (1971).
- <sup>29</sup>R. C. A. Brown, H. J. Hilke, and P. Jarman, Nature **220**, 1177 (1968).
- <sup>30</sup>R. C. A. Brown, H. J. Hilke, and P. Jarman, Preprint CERN, D.Ph. 11/USBC 70-2 (1970).
- <sup>31</sup>R. C. A. Brown *et al.*, in: Proc. Intern. Conf. Bubble Chamber Technology, Argonne Natl. Lab. (1970), p. 376.



- <sup>32</sup>V. A. Akulichev *et al.*, Dokl. Akad. Nauk SSSR **189**, 973 (1969) [Sov. Phys. Dokl. **14**, 1173 (1970)]; Akust. Zhurn. **15**, 505 (1969).
- <sup>33</sup>V. A. Akulichev *et al.*, Soobshchenie (Communication), JINR, R13-6513 (1972); Akust. Zhurn. **19**, 486 (1973).
- <sup>34</sup>R. C. A. Brown, G. Harigel, and H. J. Hilke, Nucl. Instrum. Methods **82**, 327 (1970).
- <sup>35</sup>V. A. Akulichev *et al.*, Soobshchenie (Communication), JINR, R13-7474 (1973); Dokl. Akad. Nauk SSSR **216**, 517 (1974) [Sov. Phys. Dokl. **19**, 297 (1974)].
- <sup>36</sup>W. P. Mason (ed.), Physical Acoustics, Vol. 1A, Academic Press, New York (1964).
- <sup>37</sup>L. O. Makarov, in: 7th Intern. Congress on Acoustics, Rep. 23E6, Budapest (1971).
- <sup>38</sup>R. C. A. Brown and H. J. Hilke, Phys. Bull. **23**, 215 (1971).
- <sup>39</sup>R. C. A. Brown, H. J. Hilke, and P. D. Jarman, Nucl. Instrum. Methods **106**, 573 (1973).
- <sup>40</sup>T. D. Blakhintseva *et al.*, Prib. Tekh. Eksp. **5**, 51 (1962).
- <sup>41</sup>N. Ishihara *et al.*, Jpn. J. Appl. Phys. **14**, 101 (1975).
- <sup>42</sup>V. A. Akulichev and A. M. Kopova, in: VIII Vsesoyuznaya Akusticheskaya Konferentsiya (Eighth All-Union Acoustics Conference), Acoustics Institute, Moscow (1973).
- <sup>43</sup>L. D. Landau and E. M. Lifshits, Mekhanika Sploshnykh Sred [Mechanics of Continuous Media, Pergamon Press, Oxford (1960)], Fizmatgiz, Moscow (1954).
- <sup>44</sup>V. A. Akulichev *et al.*, in: Intern. Conf. Instrum. for High Energy Physics, Frascati, Italy (1973), p. 41.
- <sup>45</sup>R. C. A. Brown, H. J. Hilke, and P. D. Jarman, in: Intern. Conf. Instrum. for High Energy Physics, Frascati, Italy (1973), p. 38.
- <sup>46</sup>M. S. Plesset and S. A. Zwick, J. Appl. Phys. **25**, 493 (1954).
- <sup>47</sup>G. T. Trammell, J. Appl. Phys. **33**, 1662 (1962).
- <sup>48</sup>V. A. Akulichev *et al.*, Soobshchenie (Communication), JINR, R13-5327 (1970).
- <sup>49</sup>V. A. Akulichev, V. N. Alekseev, and K. A. Naugol'nykh, Akust. Zhurn. **17**, 356 (1971).
- <sup>50</sup>L. G. Tkachev and V. D. Shestakov, Akust. Zhurn. **18**, 433 (1972).
- <sup>51</sup>L. G. Tkachev and V. D. Shestakov, Akust. Zhurn. **19**, 257 (1973).
- <sup>52</sup>V. A. Akulichev and V. N. Alekseev, in: Otchet Akusticheskogo In-Ta (Report of the Acoustics Institute), Moscow (1973).
- <sup>53</sup>V. N. Alekseev, in: VIII Vsesoyuznaya Akusticheskaya Konferentsiya (Eighth All-Union Acoustics Conference), Acoustics Institute, Moscow (1973).
- <sup>54</sup>V. A. Akulichev, Akust. Zhurn. **21**, 351 (1975).
- <sup>55</sup>V. N. Alekseev, Akust. Zhurn. **21**, 497 (1975).
- <sup>56</sup>V. D. Shestakov and L. G. Tkachev, Intern. J. Heat Mass Transfer **18**, 685 (1975).
- <sup>57</sup>L. G. Tkachev and V. D. Shestakov, in: VI Mezhdunar. Simpozium po Nelineinoi Akustike (Sixth Intern. Symposium on Nonlinear Acoustics), Izd-vo MGU, Moscow (1975), p. 282.
- <sup>58</sup>A. Yu. Didyk, L. G. Tkachev, and V. D. Shestakov, in: Simpozium po Fizike Akustiko-Gidrodinamicheskikh Yavlenii, Sukhumi (Symposium on the Physics of Acoustico-Hydrodynamic Phenomena, Sukhumi), Nauka, Moscow (1975), p. 107.
- <sup>59</sup>V. A. Akulichev, V. N. Alekseev, and V. P. Yushin, in: Simpozium po Fizike Akustiko-Gidrodinamicheskikh Yavlenii, Sukhumi (Symposium on the Physics of Acoustico-Hydrodynamic Phenomena, Sukhumi), Nauka, Moscow (1975), p. 80.
- <sup>60</sup>V. N. Alekseev, Akust. Zhurn. **22**, 185 (1976).
- <sup>61</sup>V. A. Akulichev, V. N. Alekseev, and V. P. Yushin, in: Otchet Akusticheskogo In-Ta (Report of the Acoustics Institute), Moscow (1975).
- <sup>62</sup>V. A. Akulichev, V. N. Alekseev, and V. P. Yushin, in: VI Mezhdunar. Simpozium po Nelineinoi Akustike (Sixth Intern. Symposium on Nonlinear Acoustics), Izd-vo MGU, Moscow (1975), p. 262.
- <sup>63</sup>A. Yu. Didyk, L. G. Tkachev, and V. D. Shestakov, Soobshchenie (Communication), JINR R13-9458, Dubna (1976).
- <sup>64</sup>M. S. Plesset and D.-Y. Hsieh, Phys. Fluids **3**, 882 (1960).
- <sup>65</sup>A. Eller and H. G. Flynn, J. Acoust. Soc. Amer. **37**, 493 (1965).
- <sup>66</sup>T. Wang, J. Acoust. Soc. Amer. **50**, 1131 (1974).
- <sup>67</sup>L. G. Tkachev and V. D. Shestakov, Soobshchenie (Communication), JINR R13-7206 (1973).
- <sup>68</sup>G. Harigel, G. Horlitz, and S. Wolff, Report DESY, 72/16, Hamburg (1972).
- <sup>69</sup>O. A. Kapustina and Yu. G. Statnikov, Akust. Zhurn. **13**, 383 (1967).
- <sup>70</sup>L. R. Turner, Report at Meeting on USBC, Rutherford High Energy Labor. (1971).
- <sup>71</sup>V. A. Akulichev *et al.*, Avt. Svid. (Author's Certificate), No. 275243, Byull. Izobretenii, No. 29 (1974).

Translated by Julian B. Barbour